







Article

A Joint Approach of Morphological and UHPLC-HRMS Analyses to Throw Light on the Autochthonous ‘Verdole’ Chestnut for Nutraceutical Innovation of Its Waste

Elvira Ferrara ^{1,2,†}, Maria Tommasina Pecoraro ^{1,2,†} , Danilo Cice ² , Simona Piccolella ¹ ,
Marialuisa Formato ¹ , Assunta Esposito ¹ , Milena Petriccione ^{2,*} and Severina Pacifico ¹ 

- ¹ Dipartimento di Scienze e Tecnologie Ambientali Biologiche e Farmaceutiche, Università degli Studi della Campania “Luigi Vanvitelli” Via Vivaldi 43, 81100 Caserta, Italy
² CREA-Centro di Ricerca Olivicoltura, Frutticoltura e Agrumicoltura, Via Torrino 3, 81100 Caserta, Italy
* Correspondence: milena.petriccione@crea.gov.it
† These authors contributed equally to this work.

Abstract: Nowadays, chestnut by-products are gaining a lot of interest as a low-cost raw material, exploitable for developing added-value products. This is in line with suitable chestnut by-products’ management, aimed at reducing the environmental impact, thus improving the chestnut industry’s competitiveness and economic sustainability. In this context, with the aim of valorizing local cultivars of European chestnuts (*Castanea sativa* Mill.), our attention focused on the Verdole cultivar, which has been characterized by using the UPOV guidelines for its distinctness, homogeneity, and stability. After harvesting, Verdole chestnuts were properly dissected to collect the outer and inner shells, and epispem. Each chestnut part, previously crushed, shredded, and passed through diverse sieves, underwent ultrasound-assisted extraction. The extracts obtained were evaluated for their total phenolic, flavonoid, and tannin content. The antiradical capacity by DPPH and ABTS assays, and the Fe(III) reducing power, were also evaluated. Although all the samples showed dose-dependent antioxidant efficacy, plant matrix size strongly impacted on extraction efficiency. LC-HRMS-based metabolic profiling highlighted the occurrence of different polyphenol subclasses, whose quantitative ratio varied among the chestnut parts investigated. The outer shell was more chemically rich than inner shell and epispem, according to its pronounced antioxidant activity. The polyphenol diversity of Verdole by-products is a resource not intended for disposal, applicable in the nutraceutical sector, thus realizing a new scenario in processing chestnut waste.

Keywords: European chestnut; polyphenols; LC-HR MS/MS; waste management; circular economy; green extraction



Citation: Ferrara, E.; Pecoraro, M.T.; Cice, D.; Piccolella, S.; Formato, M.; Esposito, A.; Petriccione, M.; Pacifico, S. A Joint Approach of Morphological and UHPLC-HRMS Analyses to Throw Light on the Autochthonous ‘Verdole’ Chestnut for Nutraceutical Innovation of Its Waste. *Molecules* **2022**, *27*, 8924. <https://doi.org/10.3390/molecules27248924>

Academic Editor: Maria Atanassova

Received: 30 November 2022

Accepted: 13 December 2022

Published: 15 December 2022

Publisher’s Note: MDPI stays neutral with regard to jurisdictional claims in published maps and institutional affiliations.



Copyright: © 2022 by the authors. Licensee MDPI, Basel, Switzerland. This article is an open access article distributed under the terms and conditions of the Creative Commons Attribution (CC BY) license (<https://creativecommons.org/licenses/by/4.0/>).

1. Introduction

The sweet European chestnut (*Castanea sativa* Mill.), belonging to the Fagaceae family, is widely distributed in Europe with an invaluable cultural and historical heritage [1,2], so much so that its importance in the traditional economy has been referred to as “chestnut civilization” [3]. Thanks to its eco-pedological characteristics, it is appropriate for sustainable cultivation in hilly and mountain areas, providing the valorization of these marginal landscapes [4]. As the species plays an important role in the economic and environmental context of the food and wood industry, nowadays a new turning point leads to a revival in *C. sativa* cultivation [5]. Thus, the world production of chestnuts is growing, especially thanks to the high nutritional power of its fruit, suitable for consumption by non-celiac people sensitive to gluten and as an ingredient in health-related food products [6,7]. Around 2.3 million tons of fresh fruit were produced worldwide in 2020. China is the largest chestnut producer with 1.74 million tons, followed by Spain with 188,690 tons and Bolivia

with 80,882 tons. Italy is the sixth largest producer in the world and the second in Europe with production of 49,750 tons [8].

This production is connected to a large number of chestnut shells which represent underutilized agricultural and forestry waste that can be exploited as a significant resource for the production of high-value natural active compounds [9,10]. In fact, as is known, the chestnut is covered with a shell that represents about 20% of its weight which is removed during the peeling process [11]. The removal of the shell, which is composed of the pericarp (outer shell), integument (inner shell), and episperm [12], produces multiple agro-residues that can be differently exploited for the extraction of high added-value bioactive compounds [10] and recyclable in different application fields (e.g., for fertilizing and feeding animals) [13–15]. In fact, low-molecular-weight phenols, such as gallic acid and protocatechuic acid [16,17], as well as hydrolysable and condensed tannins, and flavonoids have been found as constituents of chestnut shells [11,16,18–21], although an high variability in phenol content was found, ranging from 2.7 to 5.2% [20]. It is certain that the type of cultivar in the first place and then the soil and climatic conditions of cultivation, the harvest time, as well as the extraction conditions can massively influence the content of polyphenolic compounds [22,23]. Moreover, a polysaccharide portion can also be recovered from the chestnut shell. The abundance of these substances increases the value of the shells, and emphasizes, together with the presence of antioxidants, the potential benefits of designing high-added-value products with a circular economy approach [24].

In Campania, the first Italian region for chestnut groves with 13,800 hectares and an increase of 20–30% in areas destined for chestnut groves in recent years [25], chestnut cultivation is of considerable economic and social importance not only for fruit and wood production, but also for the conservation and hydrogeological landscape protection [26].

The recent certification of Marrone/Castagna di Serino PGI (Protected Geographical Indication) [27] has further innovated the chestnut production of the Campania Region with fruits of high-quality characteristics. In fact, Marrone/Castagna di Serino designates the fresh, peeled, dried in-shell, and whole dried shelled fruit of two varieties from European chestnut species: the ‘Montemarano’ variety, also referred to as ‘Santimango’, ‘Santomango’, ‘Marrone di Avellino’ or ‘Marrone avellinese’, and the ‘Verdola’ or ‘Verdole’ local variety. The Verdole variety, which also makes up 10% of the ‘Castagna di Montella’ PGI [28], and acts as a pollinator variety for its resistance to adverse environmental conditions and cryptogams, is the main chestnut cultivar grown in many low-altitude valleys near Serino (Avellino province). This makes this autochthonous variety a widely consumed product at a local level. Since the transformation of chestnuts leads to the production of an enormous quantity of waste and by-products, with a view to outlining new directions of use for local producers and the establishment of self-powered and sustainable supply chains, the study of phytochemistry has been carried out on the composition of the non-organic edible components of the Verdole cultivar. In addition to providing a series of guides and information for the distinctness, uniformity, and stability of Verdole chestnuts, traits of phenological and morphological characters have been evaluated.

Hence, in response to the current perspective of containment of agro-industrial waste, through the increase in the sustainability of production and the activation of an economic circularity of the company [29], the phytochemical study of the different components of the shell of the Verdole cultivar represents the first step for an effective enhancement of resources. For this purpose, samples of chestnuts of the Verdole variety have been collected and shelled. The shells, further separated into different components, have been subjected to differential pulverization procedures, and extracted by ultrasound-accelerated maceration using ethanol. The total content of condensed tannins, and the total content of flavonoids and phenols, as well as the anti-radical capacity, have been evaluated in each shell component. Furthermore, the relative metabolic profile has been recorded by means of a non-targeted Ultra-High Performance Liquid Chromatography–High Resolution Mass Spectrometry (UHPLC-HRMS).

2. Results and Discussion

2.1. Morphological Analysis









Castanea sativa cv. Verdole was described using forty-seven morphological traits-descriptor for carrying out tests of the distinctness, homogeneity, and stability of chestnut established by the Union for the Protection of New Varieties of Plants (UPOV) guidelines (TG/124/4—UPOV 2017) [30]. For each mean value obtained, a state and numerical number were assigned using the UPOV as reported in Table S1 (Supplementary Materials). Verdole is a native variety of Campania Region and, as reported in Tables 1 and S1, with medium tree vigor and upright habit. The bud of the current season is dense with long internodes and opposite leaf arrangements. Each shoot contains many female flowers and very long male flowers (catkins). The leaves are large and moderately asymmetrical with a slightly concave profile in cross-section. The top side shows a medium intensity of green color while the bottom side appears as light green. The shape of a leaf is narrow and elliptical with a sharp apex and a corded base. The burrs have an obloid shape with a low density of thorns and contain two or three fruits. It produces a red-brown colored nut with a single embryonic seed and medium penetration of the epidermis. With regard to pomological traits, according to Figure 1A the box indicates the 25th and 75th percentiles and the whiskers represent the maximum and minimum values of fruits. The fruits' average weight is $12.2 \text{ g} \pm 2.3$ with the fruits' width and height of $32.6 \pm 2.6 \text{ mm}$ and $29.5 \pm 1.6 \text{ mm}$, respectively. The hilum height and length are $12.3 \pm 1.3 \text{ mm}$ and $22.3 \pm 3.1 \text{ mm}$, respectively. The style and the flower remaining part show a height of $6.3 \pm 1.2 \text{ mm}$, while the seeds evidence the adherence to the core and the yellowish color of the pulp. This variety has a medium-term leaf budding and the early male flowering-period and the average female flowering ripening-period occurs towards the end of September and can be considered medium. Fruit is suitable for fresh consumption due to its organoleptic and sensorial characteristics. Many of these characteristics are stable and the evaluation of a single year in a single site is satisfactory, as already demonstrated on observations carried out on thirty-eight traditional chestnut cultivars from a contemporary collection in the northwest of the Iberian peninsula [31]. On the contrary, phenological parameters (time of leaf bud burst, time of beginning of male and female flowering) and one related to fruit size (size of fruit hilum) need to be evaluated under contrasting site conditions for a minimum number of years as it has been demonstrated that they can vary in relation to environmental conditions [31,32].

Herein, for a greater and more in-depth detail of the characteristics of the fruit, the individual components of the integument and the seed were accurately dissected. Verdole cv. chestnuts were shelled, and shells acquired were dissected in its outer and inner part, as well as episperm (Figure 1B). It was found that, in addition to the edible seed which was 83.2%, the outer shell accounted for 8.6%, the inner shell 1.8%, and the episperm for 6.4%.

2.2. Extraction of Chestnut Fruits

The extraction method mostly affects the recovery of bioactive compounds from plant matrices [33]. Several parameters, such as solid–liquid ratio, particle sizes, solvent polarity, temperature, extraction time, and pH impacted on the extraction efficiency [18,34–36]. The literature data highlighted that different extraction methods were applied to chestnut shells [18]. As a result, significant differences in the qualitative and quantitative phenolic patterns of chestnuts shells were found. The large amount of literature data clashed with the scarce information relating to the cultivar, the geographical origin, and the collection site of the chestnuts whose shell polyphenolic component was studied. The chestnut shell represents a processing waste for the processing industries that must be disposed of, where it could generate new economic and social profit [37]. Table 2 shows the literature search of different papers that used chestnut shells as the starting matrix.

Table 1. *Castanea sativa* cv. Verdole morphological traits according to UPOV guideline.

VERDOLE DESCRIPTOR ATTRIBUTED		
	Tree: vigor Tree: growth habit	<i>Medium</i> <i>Upright</i>
	Current season's shoot: thickness Current season's shoot: length of internodes Current season's shoot: arrangement of leaves Current season's shoot: color of upper side stem Current season's shoot: density of lenticels Shoot: number of female flowers	<i>Thick</i> <i>Long</i> <i>Opposite</i> <i>Yellow brown</i> <i>Dense</i> <i>Many</i>
	Male flower: length of filament Catkin: length	<i>Very long</i> <i>Long</i>
	Young leaf: bronze coloration Leaf: size Leaf: profile in cross-section Leaf: symmetry Leaf: length/width ratio Leaf: attitude in relation to shoot Leaf blade: green color intensity of upper side Leaf: color of lower side Leaf: shape Leaf: shape of apex Leaf: the shape of base Leaf: shape of margin Leaf: symmetry of base Leaf: color of petiole Leaf: ratio length of leaf blade/length of petiole	<i>Absent</i> <i>Large</i> <i>Slightly concave</i> <i>Moderately asymmetric</i> <i>High</i> <i>Upwards</i> <i>Medium</i> <i>Light green</i> <i>Narrow elliptic</i> <i>Broad acuminate</i> <i>Cordate</i> <i>Acute</i> <i>Symmetric or slightly asymmetric</i> <i>Green</i> <i>High</i>
	Bur: shape Bur: density of prickles	<i>Obloid</i> <i>Sparse</i>
	Nut: embryony Nut: degree of seed coat penetration into embryo Nut: shape Nut: area of pubescence on upper part Nut: area of hilum Nut: shape of border line of hilum and pericarp Nut: conspicuousness of hilum Nut: glossiness Nut: color of skin Nut: size	<i>Mono-embryonic</i> <i>Medium</i> <i>Circular</i> <i>Small</i> <i>Small</i> <i>Wavy</i> <i>Conspicuous</i> <i>Present</i> <i>Reddish brown</i> <i>Medium</i>
	Seed coat: adherence to kernel Kernel: color of flesh	<i>Weak</i> <i>Yellow</i>
	Time of leaf bud burst Time of male flowering Time of female flowering Time of maturity for consumption	<i>Medium</i> <i>Early</i> <i>Medium</i> <i>Early</i>

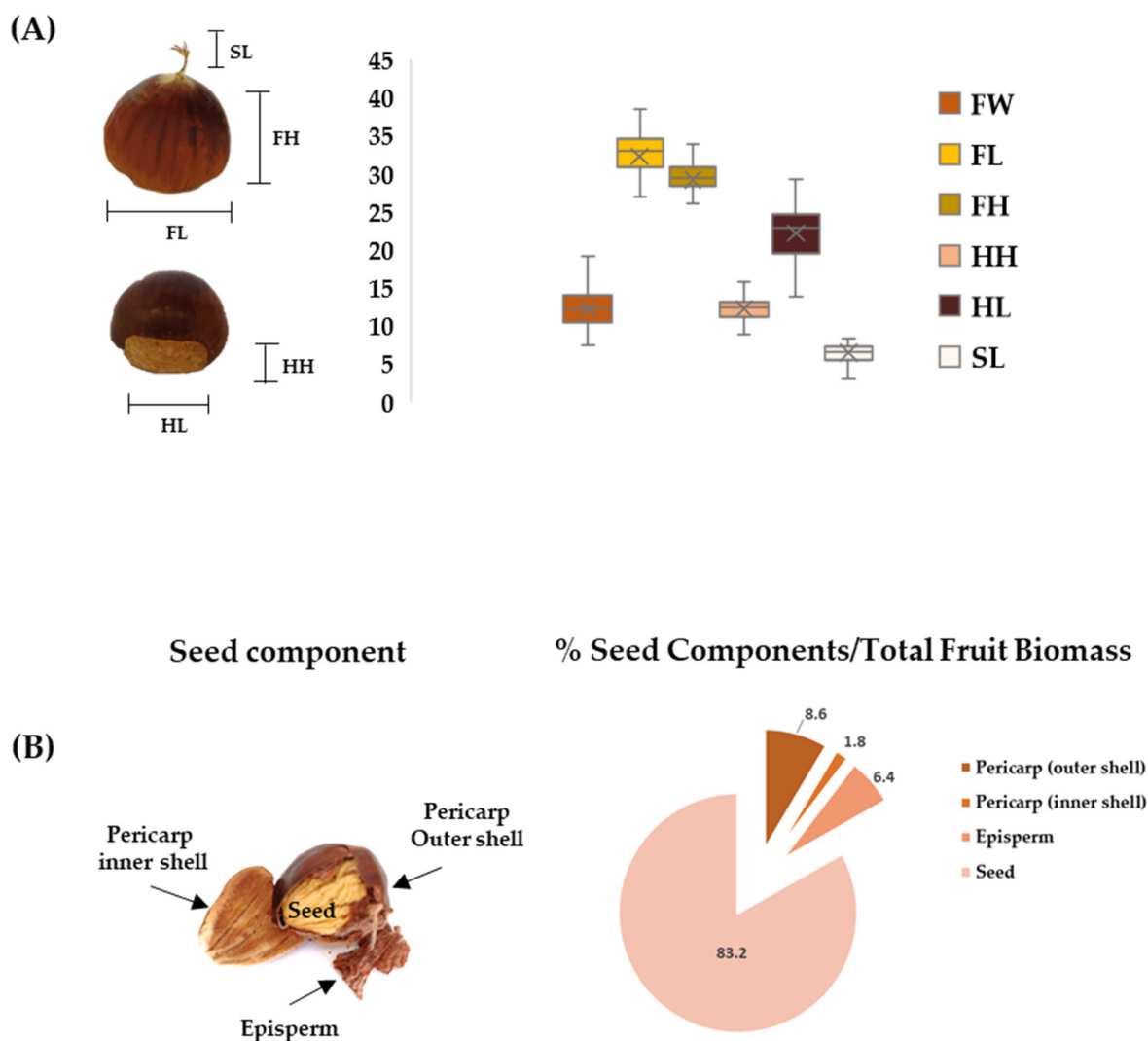


Figure 1. (A) Box and whiskers plot of the average values of morphological traits measures ($n = 100$) of chestnut fruit (FW: Fruit Weight; FL: Fruit Length; FH: Fruit Height; HH: Hilum Height; HL: Hilum Length; SL: Style Length). (B) Fruit components with relative %—Average Biomass (dry weight; $n = 100$ fruits).

Starting from recovered Verdole cv. chestnut shells, the impact of particle size on extraction efficiency was preliminarily investigated, and the use of sieves was designed to prepare sequentially four outer shell matrices (P_{os1} – P_{os4}). The latter were obtained in the relative percentage of 47.5% (P_{os1}), 21.6% (P_{os2}), 7.9% (P_{os3}), and 4.3% (P_{os4}) with respect to the previously shredded outer-shell matrix. Thus, each component underwent extraction using ultrasound-assisted maceration and ethanol as an extractant.

The reduction of the matrix to fine powders was in line with the relative increase in the specific surface area and appeared to be a guarantee for effective diffusion of the solvent within the matrix and greater mass transfer. Indeed, considering the percentage data from the shredded outer shell matrix, while observing that the extraction efficiency for the same weight of the differently sieved initial matrix increased with the decrease in the particle size, passing from 1.7% (P_{os1}) to 5.7% (P_{os4}), it is assumed that the processing of outer shell with particles larger than 1 mm, leads to a good recovery of bioactive compounds (Figure 2B).

Table 2. Collection site cultivar and supplier, extraction methods and solvents, analytical tools used for chestnut shells' characterization. TPP = Total Phenol Content; TFC = Total Flavonoid Content; TcTC = Total condensed Tannin Content; AA = Antioxidant Activity; EtOH = ethanol; MeOH = methanol; PET = Petroleum Ether; RT = Room Temperature; UAM = Ultrasound Assisted Maceration; SWE = Supercritical Water Extraction.

Cultivar	State	Extraction Method	Extraction Solvent	Analytical Tools	TPC	TFC	TcTC	AA	Refs.
–	Italy	Maceration (Ø 1–2 mm)	EtOH: H ₂ O (different ratios <i>v:v</i>)	HPLC-UV-VIS	X	x			[22]
–	Spain	Acid hydrolysis (Ø 0.4 mm)	–	FTIR; TGA; MALDI-TOF-MS	X	x		x	[38]
Marrone di Roccadaspide	Italy	Maceration (RT)	MeOH, PET, CHCl ₃	LC-ESI/QTrap/MS ⁿ	X	x	x	x	[39]
–	Spain	Soxhlet	Several solvents	FT-IR; UV/Vis	X			x	[40]
–	Italy	SWE	H ₂ O	LC-DAD/ESI-MS	X			x	[37]
–	Portugal	UAM	H ₂ O	LC-UV-MS; ¹ H NMR	X			x	[41]
–	Portugal	Microwave	EtOH: H ₂ O (different ratios, <i>v:v</i>)	LC-ESI/MS	x	x		x	[42]
–	Italy	Decoction	Boiling H ₂ O (1 h)	UHPLC-MS/MS	x		x		[43]
Palomina	Italy	Ultra Turrax homogenizer; Decoction	Boiling H ₂ O (30 min)	HPLC-UV	x			x	[44]
–	Spain	N.I.H	Alkaline solution or H ₂ O	HPLC	x			x	[45]
–	Italy	Maceration (RT)	MeOH (60%—1:10, <i>w:v</i>); EtOH (60%—1:10, <i>w:v</i>); H ₂ O (1:40, <i>w:v</i>)	HPLC-DAD	x		x	x	[46]
–	–	UAM (59 kHz)	EtOH: H ₂ O (7:3, <i>v:v</i>)	HPLC-MS/MS	x	x		x	[47]
–	Bosnia	UAM (50 Hz and 125 W)	EtOH	–	x	x	x		[48]
Napoletana; Mercogliana Tempestiva; Bouche	Italy	Decoction	Boiling H ₂ O (40 min)	HPLC-UV-DAD	x	x		x	[49]
–	Portugal	Maceration (RT)	EtOH	HPLC-DAD/ESI-MS	x		x	x	[50]
–	Italy	Maceration	Boiling H ₂ O (1 h)		x	x	x	x	[16]
Judia		Maceration	EtOH	HPLC-UV	x	x	x		[51]
–	Italy	UAM (35 kHz)	MeOH	HPLC DAD/ESI-MS	x		x		[52]
–	Italy	–	MeOH (after defatting) EtOH:H ₂ O (1:1, <i>v:v</i>)	UHPLC-UV/ESI-HRMS	x			x	[53]

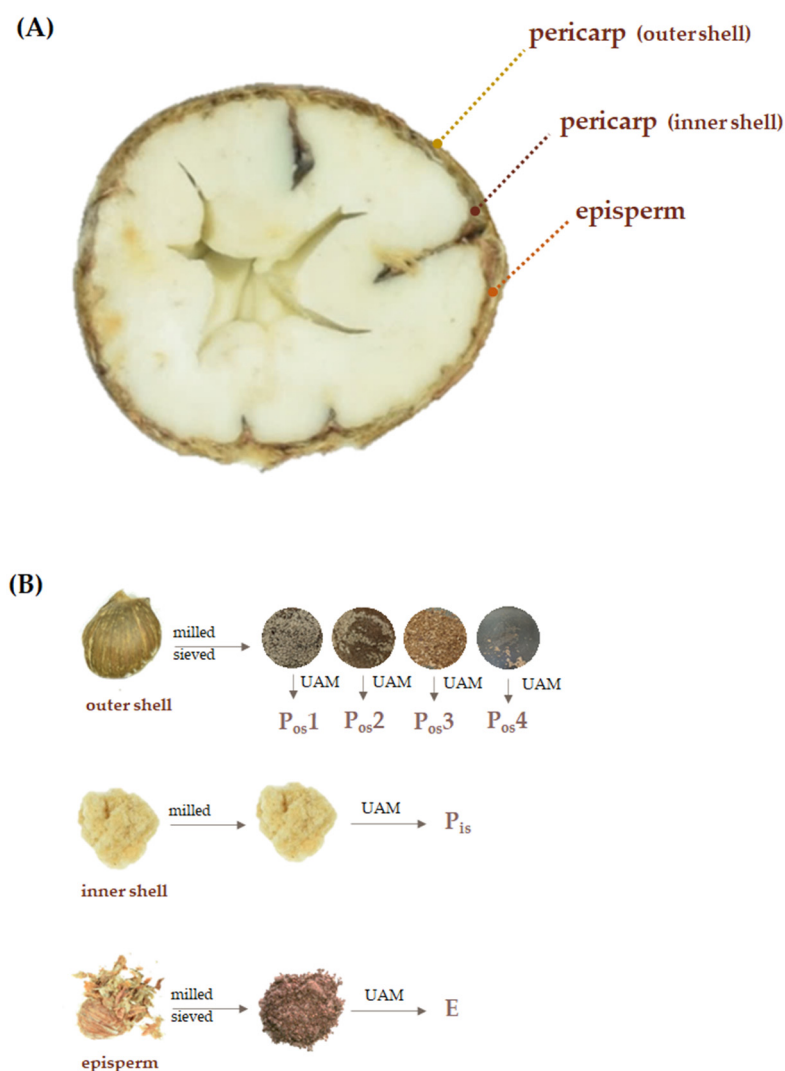


Figure 2. (A) Cross dissection of chestnut fruit; (B) Separation of the outer shell, inner shell, and episperm from the seed. Outer shell was sieved and different granulometric fractions were obtained. All the fractions underwent UAM (Ultrasound Assisted Maceration) using ethanol.

2.3. Shell Components Differ in Phenols and Flavonoids, and Otherwise Act as Antioxidants

The different components of the chestnut shell of the cultivar Verdole were investigated in terms of total phenols (TPC), total flavonoids (TFC), and total condensed tannins (TcTC) (Figure 3). The anti-radical and Fe(III) reducing efficacy was also evaluated. The Principal Component Analysis of the data matrix performed with the values of the parameters showed, above all, a significant difference between the type of matrices examined. Episperm was at the positive end of the first axis, which reaches a dissimilarity value of 81.22%. On the contrary, the outer shell samples were pooled in the negative score. In particular, the P_{os4} extract showed a positive correlation with TPC and TcTC labels, whereas P_{os3} and P_{os2} appeared to be positively correlated with flavonoid content (TFC).

The data were compared with those already present in the literature for this type of processing waste. Condensed tannins, ellagitannins, phenolic acids, and flavonoids are reported as the main constituents [42], to which health-promoting effects against oxidative stress-related disorders are attributed [54]. In this context, it was observed that the alcoholic extracts from the differently sieved outer shell, were able to scavenge stable radicals, such as the DPPH• and ABTS•⁺, whereas extracts from the inner shell and episperm were inefficient to reduce DPPH radical and exerted an ABTS•⁺ scavenging capability six-fold lower than that from P_{os1}. This latter scavenged both the radical species less than extracts obtained using

sieves with smaller meshes. Data from the ferricyanide FRAP assay highlighted that all the extracts contained compounds able to transfer a single electron to ferric ions.

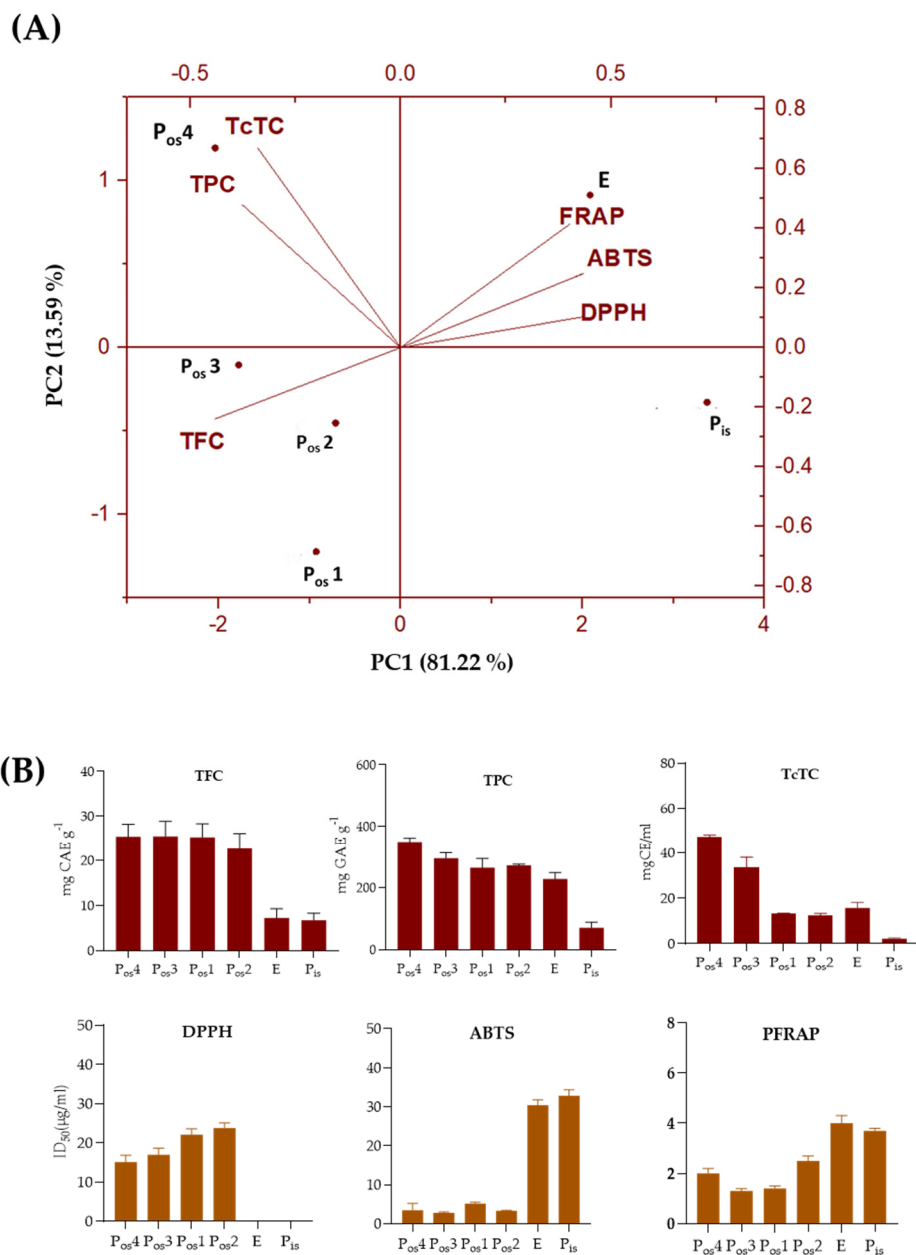


Figure 3. (A) PCA of antioxidant assays (DPPH, ABTS, and ferricyanide FRAP) and total content in phenols (TPC), flavonoids (TFC), and condensed tannins (TcTC) of the sampled shell components. Data processing was performed using OriginPro 2015 software. (B) Data of antioxidant assays, phenols, flavonoids, and condensed tannins of the analyzed shell components are ordered according to the gradient of the first axis (performed by GraphPad Prism 8.4.2.).

The polyphenol content (TPC), evaluated by the Folin–Ciocalteu test, ranged between 393.42 mg GAE/g DW in the outer shell and 70.19 mg GAE/g DW in the inner shell, while the TPC of the chestnut episperm was 227.43 mg GAE/g DW (Figure 3B). This finding was in line with previous findings related to the non-uniformity of the distribution of phenolic compounds in plants. Typically, the outer layers contained higher levels of phenols than the inner ones [55].

Particle size fractionation was effective in producing four powdered outer shell materials with an average phenol and flavonoid content of 294.54 mg GAE/g DW and 24.71 mg EC/g

DW, respectively. The results acquired were comparable to the polyphenol content in the *C. sativa* shell extract obtained using ultrasound-assisted extraction at 70 °C for 40 min (393.1 mg GAE/g DW) [41], subcritical water extraction (315.21 mg GAE/g DW to 496.80 mg GAE/g DW) [42], and conventional extraction methodologies [14,40,56]. Higher TPCs were obtained in the MeOH and EtOH shell extracts of Italian chestnut cultivars with values of 870.81 mg GAE per gram of extract and 547.85 mg GAE per gram of extract, respectively [39]. Lower TPC values were obtained from the outer shell when treated with aqueous alkaline solvents [16,46] or with organic solvents of different polarity [41,46,57].

The chestnut epispem showed a higher TPC than that determined by Squillaci et al. [16] when the inner part of the shell was removed from the “Brulage” peeling process, while a higher TPC was detected in the ethanol extraction by Silva et al. [50]. The flavonoid content was higher in the outer shell and epispem than in the inner shell (Figure 3B). Previous studies reported a TFC of 6.5 mg CE/g DW and 14.4 mg CE/g DW [48], and of 7.94 mg CE/g DW and 40.98 mg CE/g DW [16] for the epispem and outer shell, respectively. A lower TFC value was reported by Hong et al. [57] for chestnut shell extract including internal and external shells. Pinto et al. [42] found a TFC between 25.50 mg of CE/g DW and 68.56 mg of CE/g DW in the ethanolic and aqueous extract of chestnut shells, respectively. On the contrary, Vella et al. [49] determined a significantly lower TFC for the outer shell compared to the inner shell even after employing longer extraction periods and higher temperatures.

2.4. UHPLC-HR-MS/MS Analysis

According to previous findings, hexuronic acid and its derivatives were found as the main constituents of inner shell and epispem, while diverse hydrolysable and condensed tannins were detected as constituents of the investigated chestnut materials, together with flavonoid compounds [38]. This latter appeared the most abundant class in all the outer shell extracts. This could be due to the use of ethanol as an extractant.

The high content of hexuronic acid, mainly at the inner shell level, was in line with previous observations relative to the content of galacturonic acid [38]. Furthermore, investigating the monosaccharide content of the shell of four chestnut varieties (Bouche de Betizac, Marigoule, Goujounac, and Bournette), it was found that xylose and galacturonic acid were the most representative. Herein, the evidence of the compound was through the detection of the deprotonated molecular ion at m/z 193.0354 (compound C; Figure 4), which underwent decarboxylation to achieve the ion at m/z 149.0436, and further dehydrated twice for giving the ion at m/z 113.0251. A galacturonyl-based compound was also compound B, with relative $[M-H]^-$ ion at m/z 777.1603. This latter fragmented in the ToF-MS/MS experiment providing the main ions at m/z 583.1166, and 365.0729, according to sequential neutral losses of hexuronate, and acetyldehydrohexuronate. ToF-MS/MS data of compound A was tentatively identified as methyl 3-O-(3,6-anhydrohexopyranosyl) hexopyranoside.

Galacturonic acid is a very versatile compound used extensively in the food industry. In fact, it acts as an acidifying agent, is a good sequestering agent, and was proposed as an ingredient in cosmetics and pharmaceuticals. Recently, PCS-2A, a polysaccharide with 62.8% galacturonic acid, was isolated from the chestnut shell, and this high rate of galacturonic acid was due to its antioxidant capacity, and hepatoprotective effects [58]. Dietary pectin represents the main source of galacturonic acid [59], and its benefits appeared to ameliorate the intestinal mucosal permeability and inflammation of functional dyspepsia [60]. Considering the many uses in which galacturonic acid is involved, which is also a precursor in the synthesis of vitamin C, the recovery of galacturonic acid is of great interest [61] and the chestnut inner shell is a precious resource. In fact, among the constituents detected in this waste part, it represented more than 80%.

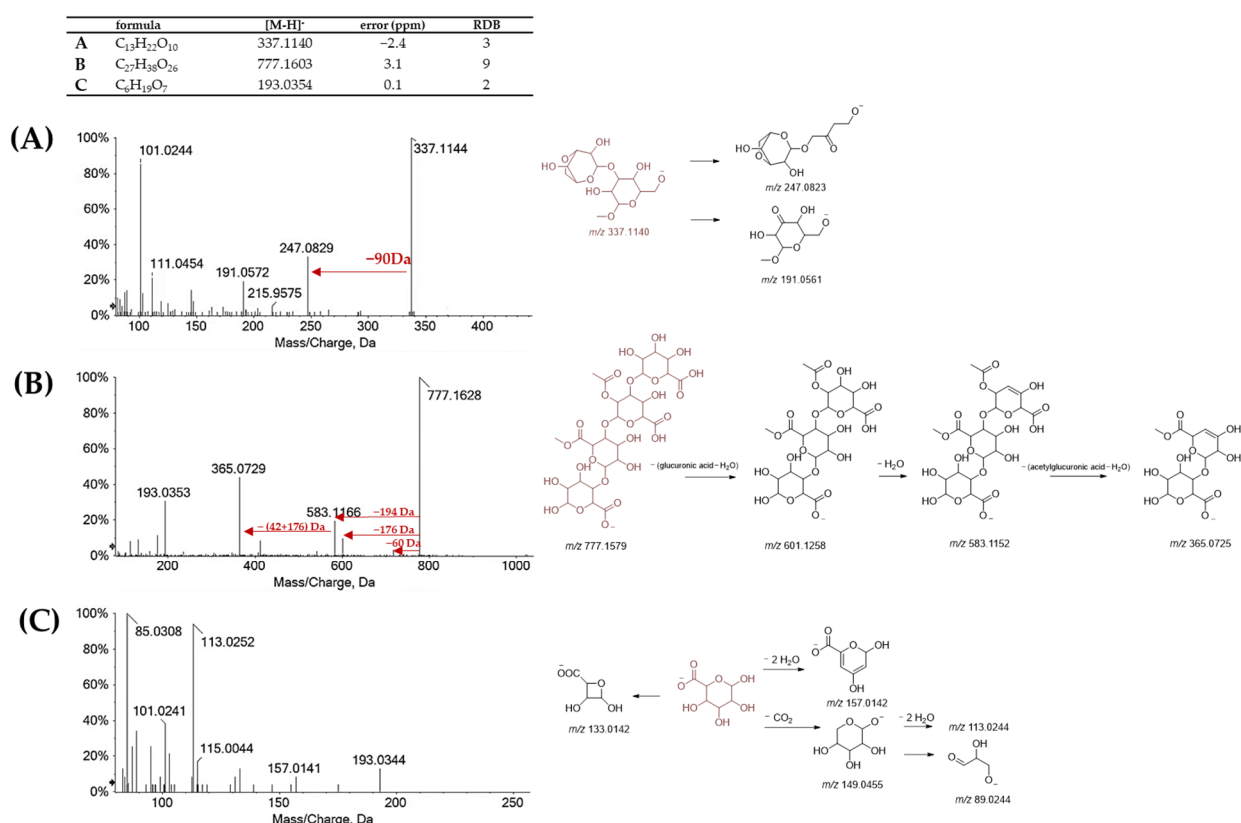


Figure 4. ToF-MS/MS spectrum of saccharidic compounds detected in inner shell and episperm extracts (A) compound A; (B) compound B; (C) compound C. Next to each spectrum, the proposed fragmentation pattern is represented. ToF-MS values, as well as RDB (ring and double bond value) and error (ppm), are tabulated.

The other shell parts, as previously described mostly accounted for tannins and flavonoids, beyond dihydroxybenzoic acid (**7**) with the [M-H]⁻ ion at m/z 153.0200, according to the molecular formula C₇H₆O₄, and the lignan hexosides, **17** and **20**. These compounds showed the deprotonated molecular ion at m/z 521.2020 and 521.2046, respectively, and ToF-MS/MS ions (at m/z 359.15, and 344.13), in accordance with the loss of dehydrated hexose. Isolariciresinol and lariciresinol glycosides were previously detected in sweet chestnut flour [62].

In Table 3, compounds, whose structure is based on gallic acid or hexahydroxydiphenic acid, are reported. In this case, the diversity in hydrolysable tannins, which are esters of gallic acid or hexahydroxydiphenic acid, is simplified in the description of the molecules of this class, mostly present in the extracts [63].

The ToF-MS and ToF-MS/MS data of compound **1** were in accordance with the hexahydroxydiphenyl hexose. In fact, the [M-H]⁻ ion at m/z 481.0634, underwent dehydrated hexose loss to achieve the ion at m/z 300.9994, which consisted of hexahydroxydiphenic acid (HHDP). Compound **4** was tentatively a galloyl derivative of compound **1**, whereas compound **9** was diHHDP-hexose, to such an extent that the dissociation of its deprotonated molecular ion at m/z 783.0709 provided the fragment ion at m/z 481.0627 in line with HHDP-hexose, and the ions at m/z 300.9984 (HHDP), and the decarboxylated HHDP ion at m/z 275.0191. Furthermore, compound **10** was also strictly related to the previous ones, being constituted by another HHDP unit. In this context, castalagin and its isomer vescalagin were previously identified as chestnut constituents [53]. These compounds were the most abundant ellagitannins in freshly felled chestnut heartwood [64]. The loss of the HHDP residue was further common to compound **31**, whose deprotonated molecular ion, after losing 302 Da, provided the ion at m/z 447.0579, which in turn lost 146.06 Da, in line with a deoxyhexose, to achieve the hexahydroxydiphenate. Compound **14** was likely castacrenin.

In fact, its deprotonated molecular ion gave the ion at m/z 493.0076 following the cleavage of the hydroxytetrahydrofuran ethanediol moiety and the loss of 120 Da. Ellagic acid (**26**) was the most abundant compound, whereas its methyl-(**41**), dimethyl (**44** and **46**), and trimethyl derivatives (**47** and **51**) were also detected. The deprotonated ion of compound **47** by losing the heptosyl unit (−192 Da) gave the deprotonated trimethylellagic acid which underwent three sequential losses of methyl radicals (Figure 5). Heptulose is a seven-carbon atoms monosaccharide, rarely found in nature [65], and herein identified for the first time as a glyconic moiety of trimethylellagic acid. This latter compound was recently investigated for its ability to exert antiproliferative activity towards different cell lines and to inhibit the growth of SW620 tumor xenografts in vivo by inducing apoptosis and anti-angiogenesis [66]. The great part of the most polar compounds in investigated chestnut shell extracts were other galloyl-based compounds. Indeed, gallic acid (**3**) and its hexoside (**2**), as well as a digalloylhexose (**15**), and two isomers of trigalloylhexose (**18** and **19**) were identified. Neutral losses of 170 and 152 Da, together with the detection of the fragment ions at m/z 169.01, and 125.02 mostly allowed the identification of these compounds. The ToF-MS/MS spectrum of the trigalloylhexose **18**, in particular, showed the deprotonated molecular ion $[M-H]^-$ at m/z 635.0890, which was beyond typical neutral losses of 152 Da and 170 Da, underwent the loss of 212 Da suggesting the location of the galloyl residues in positions 1, 3, and 5 of the saccharide portion. In fact, the 212 Da loss could be the result of a cross-link sugar cleavage (Figure 5). Compound **5** was tentatively identified as a trihydroxybenzyl alcohol hexoside, likely crenatin, previously identified as one of the main compounds of the Italian PGI chestnut ‘Marrone di Roccadaspide’ [67].

Table 3. UHPLC-ESI-QqToF/MS and MS/MS data useful for the tentative identification of compounds in chestnut extracts (base peaks in MS/MS spectra are reported in bold; RT = retention time; RDB = ring and double bond value).

Peak	RT (Min)	Tentative Assignment	Formula	$[M-H]^-$ Found (m/z)	Error (ppm)	RDB	MS/MS Fragment Ions (m/z) and Relative Intensity (%)
1	0.398	Hexahydroxydiphenyl hexose	C ₂₀ H ₁₈ O ₁₄	481.0640	3.4	12	481.0638; 300.9986 ; 275.0193; 257.0083
2	0.491	Gallic acid hexoside	C ₁₃ H ₁₆ O ₁₀	331.0663	−2.3	6	169.0137 ; 168.0073; 125.0245
3	0.674	Gallic acid	C ₇ H ₆ O ₅	169.0146	2.1	2	169.0146; 125.0248
4	0.829	Galloyl-HHDP-hexose	C ₂₇ H ₂₂ O ₁₈	633.0739	0.9	17	633.0761 ; 300.9978; 275.0193
5	0.967	Crenatin	C ₁₃ H ₁₈ O ₉	317.0886	2.5	5	317.0891; 155.0362; 137.0242
7	1.187	Dihydroxybenzoic acid	C ₇ H ₆ O ₄	153.0200	4.4	5	109.0299 ; 108.0220;
9	1.579	diHHDP-hexose	C ₃₄ H ₂₄ O ₂₂	783.0709	2.9	23	783.0707 ; 481.0627; 300.9984; 275.0191
11	1.823	Castalagin/ vescalagin	C ₃₄ H ₃₀ O ₃₁	933.0673	−2.7	20	933.0677 ; 631.0593; 300.9977
14	4.838	Castacrenin	C ₂₇ H ₁₈ O ₁₇	613.0487	2.6	10	613.0511; 493.0076 ; 300.9988
15	5.665	Digalloyl hexose	C ₂₀ H ₂₀ O ₁₄	483.0780	−0.1	11	483.0757; 313.0554; 211.0241 ; 271.0462 169.0150; 125.0250;
18	8.019	Trigalloylhexose 1	C ₂₇ H ₂₄ O ₁₈	635.0890	0	16	635.0947 ; 483.0800; 465.0701; 423.0607; 313.0567; 169.0143
19	8.085	Trigalloylhexose 2	C ₂₇ H ₂₄ O ₁₈	635.0891	0.2	16	635.0932; 589.1926; 521.2044; 465.0707 ; 359.1537; 313.0587; 169.0142
26	9.680	Ellagic acid	C ₁₄ H ₆ O ₈	300.9986	−1.3	12	301.0000 ; 283.9974; 185.0243
31	10.069	diHDDP-deoxyhexoside	C ₃₄ H ₂₂ O ₂₀	749.0643	1.5	24	447.0579 ; 300.9991; 299.9901
41	11.434	Methyl ellagic acid	C ₁₅ H ₈ O ₈	315.0145	−0.4	12.0	299.9907 ; 298.9814; 216.0057; 172.0169
44	12.245	Dimethyl ellagic acid deoxyhexoside	C ₂₂ H ₂₀ O ₁₂	475.0888	1.3	13.0	475.0912; 460.0681; 328.0228; 312.9991 ; 297.9757
46	12.855	Dimethylellagic acid	C ₁₆ H ₁₀ O ₈	329.0304	0.3	12.0	329.0307; 314.0073; 298.9837; 285.0038; 270.9887 ; 242.9934; 214.9982
47	14.272	Trimethylellagic acid eptuloside	C ₂₄ H ₂₄ O ₁₄	535.1109	2.9	13.0	343.0461; 328.0230 ; 312.9991; 297.9749
51	15.135	Trimethyl ellagic acid	C ₁₇ H ₁₂ O ₈	343.0462	0.8	12.0	312.9988; 297.9755 ; 285.0036; 269.9804; 213.9901

Proanthocyanidins, and their monomers catechin (**12**), galocatechin (**8**), and (epi)catechin gallate (**22**), were tentatively identified (Table 4). Compound **6** was likely a B-type proanthocyanidin, formed by (epi)galocatechin monomers. The deprotonated molecular ion $[M-H]^-$ at m/z 609.12 agreed with the molecular formula C₃₀H₂₆O₁₄. The neutral loss of 126 Da, consisting of the A ring loss of the monomer, supplied the ion at m/z 483 through an HRF (heterocyclic ring fission) mechanism, whereas the ion at m/z 305.0665, corresponding to the monomer unit, was formed by the mechanism of fission QM (quinone methide) with cleavage of the interflavanic bond. The loss of the B ring following a Diels Alder retro reaction confirmed the presence of the pyrogallol unit. The other three compounds (**D–F**) were found to exhibit the deprotonated molecular ion at m/z 609.125. These compounds were detected only in the episperm extract.

Compound D showed a ToF-MS/MS spectrum superimposable to that of compound 6, while compounds E and F appeared to be catechin or epicatechin derivatives.

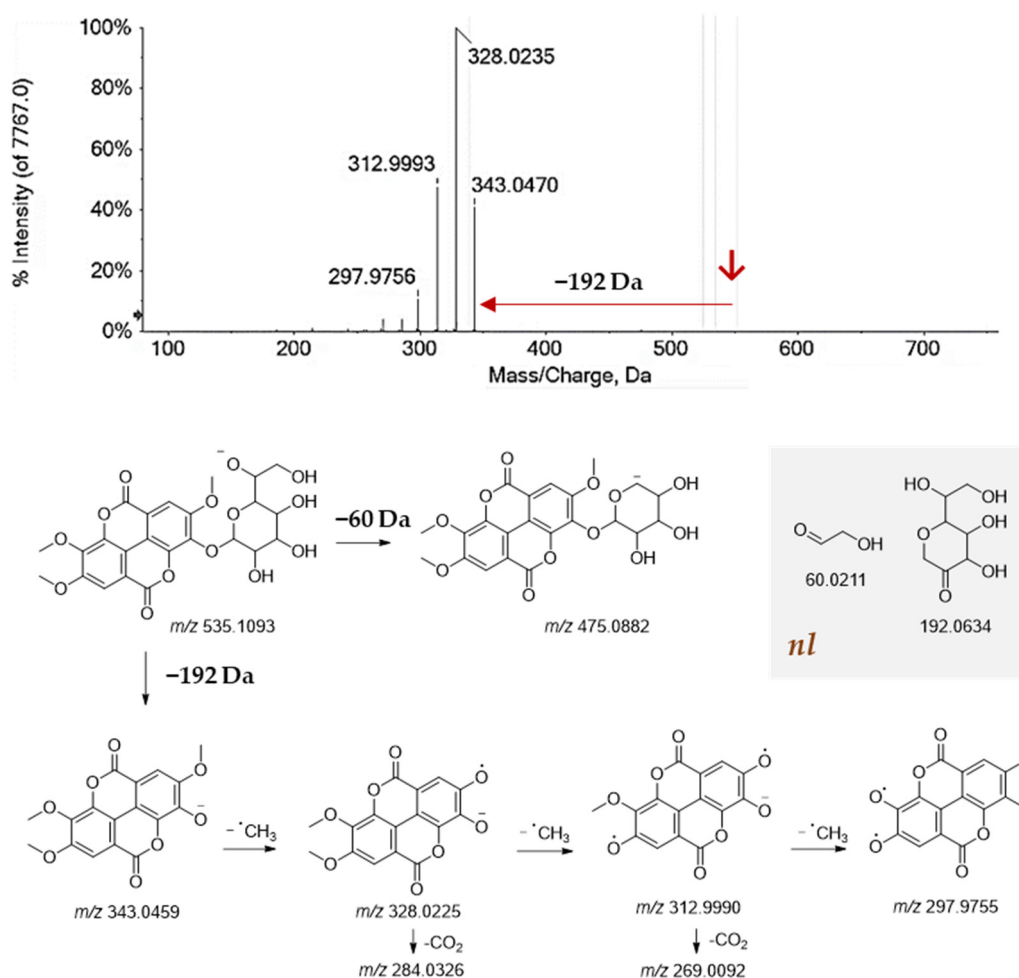


Figure 5. ToF-MS/MS spectrum of trimethylellagic heptuloside (47), and fragmentation pattern proposed. nl = neutral loss. The theoretical mass is below each structure.

Table 4. UHPLC-ESI-QqToF/MS and MS/MS data useful for the tentative identification of flavanol and proanthocyanin compounds in chestnut extracts (base peaks in MS/MS spectra are reported in bold; RT = retention time; RDB = ring and double bond value).

Peak	RT (Min)	Tentative Assignment	Formula	[M-H] ⁻ Found (m/z)	Error (ppm)	RDB	MS/MS Fragment Ions (m/z) and Relative Intensity (%)
6	1.147	Prodelfinidin B-type I	C ₃₀ H ₂₆ O ₁₄	609.1258	1.3	18	609.1278; 441.0834 ; 423.0723; 305.0664; 177.0193; 483.0942; 261.0756
D	1.308	Prodelfinidin B-type II	C ₃₀ H ₂₆ O ₁₄	609.1247	-2	18	609.1258; 441.0837; 423.0724 ; 305.0667; 177.0194
8	1.503	Gallocatechin	C ₁₅ H ₁₄ O ₇	305.0665	-0.6	9	305.0650; 261.0726; 237.0735; 219.0661; 179.0337; 167.0342; 137.0240; 125.0243 ; 111.0446
10	1.805	Procyanidin	C ₃₀ H ₂₆ O ₁₃	593.1289	-2.0	18	593.1312; 467.1045; 425.0900; 407.0795 ; 303.0546; 289.0719; 177.0202
E	2.755	(epi)Catechin derivative I	C ₃₀ H ₂₆ O ₁₄	609.1244	-1	18	609.1249; 565.1344; 457.0764; 407.0758; 319.0452; 289.0706; 275.0553 ; 231.0653; 165.0189
12	4.387	Catechin	C ₁₅ H ₁₄ O ₆	289.0719	0.5	9	289.0735; 271.0650; 245.0847; 221.0825; 205.0523; 203.0722 ; 187.0414; 175.0404; 151.0418; 137.0251; 123.0457; 109.0312
13	4.564	Procyanidin B-type	C ₃₀ H ₂₆ O ₁₂	577.1349	-0.4	18	577.1399; 451.1277; 425.0900; 407.0788 ; 289.0740; 245.0836; 125.0250
F	4.778	(epi)Catechin derivative II	C ₃₀ H ₂₆ O ₁₄	609.1245	-0.8	18	609.1257; 485.1241; 407.0771; 289.0696 ; 231.0656; 206.0667; 102.0995
16	7.229	Procyanidin A-type	C ₃₀ H ₂₄ O ₁₃	591.1158	2.3	19	591.1226; 439.0687 ; 421.0576; 285.0419; 177.0183
21	8.145	Procyanidin B-type O-gallate	C ₃₇ H ₃₀ O ₁₆	729.1475	1.9	23	729.1506 ; 577.1385; 451.1053; 425.0894; 407.0778; 289.0723; 245.0450; 125.0267
22	8.379	(epi)Catechin gallate	C ₂₂ H ₁₈ O ₁₀	441.0845	4.0	14	441.0796 ; 289.0731
32	10.073	Procyanidin B-type gallate	C ₃₇ H ₃₀ O ₁₆	729.1452	-1.2	23	729.1507; 577.1343; 407.0781 ; 289.0715; 269.0462; 125.0245

Furthermore, compound **13** was a B-type procyanidin; it shared a fragmentation pattern the same as compound **6**, showing catechin as the monomeric unit. Compounds **21** and **32** were galloyl derivatives of the B-type procyanidin.

Flavonol, flavandiol, and flavone glycosides were also found, some of which were never reported before from chestnut shells. Quercetin, isorhamnetin, and myricetin were the main flavonol aglycones (Table 5). Myricetin hexoside (**24**) and myricetin deoxyhexoside (**26**), were dihydroflavonols together, such as dihydrokaempferol glucoside (**23**) with deprotonated molecular ion at m/z 449.1097, which underwent neutral loss of 162.05 Da (to give the ion at m/z 287.0557, consisted in dihydrokaempferol) and water to achieve the base peak at m/z 269.0444. The galloyl derivative of isoquercetin (**28**) was further tentatively identified. It showed the deprotonated molecular ion at m/z 615.1050, which underwent 152 Da neutral loss to give deprotonated isoquercetin at m/z 463.0907. This latter was also identified (**30**), together with deoxyhexosyl (**35**) glycoconjugates. Dihydroquercetin (**34**) with $[M-H]^-$ ion at m/z 303.0514 was also identified, as well as its galloylhexose compound (Figure 6), likely taxillusin (**25**). In fact, when the deprotonated molecular ion dissociated the ions at m/z 491.0869 and 465.1078, through neutral losses of 126 and 152 Da, respectively, the ion at m/z 313.0584 was tentatively the galloyl hexose-H₂O residue, while that at m/z 303.0520 corresponded to dihydroquercetin. Several studies stated that dihydroquercetin exerts an Nrf2/HO-1-mediated anti-inflammatory effect and shows also hepatoprotective, cardioprotective, and neuroprotective activity [68].

Table 5. UHPLC-ESI-QqToF/MS and MS/MS data useful for the tentative identification of flavonoids in chestnut extracts (base peaks in MS/MS spectra are reported in bold; RT = retention time; RDB = ring and double bond value).

Peak	RT (Min)	Tentative Assignment	Formula	$[M-H]^-$ Found (m/z)	Error (ppm)	RDB	MS/MS Fragment Ions (m/z) and Relative Intensity (%)
23	8.842	Dihydrokaempferol deoxyhexoside	C ₂₁ H ₂₂ O ₁₁	449.1097	1.7	11	449.1094; 287.0557; 269.0444 ; 151.0035
24	9.395	Myricetin hexoside	C ₂₁ H ₂₀ O ₁₃	479.0827	−0.9	12	479.0871; 317.0336; 316.0234 ; 287.0219
25	9.494	Dihydroquercetin galloyl hexoside (e.g., taxillusin)	C ₂₈ H ₂₆ O ₁₆	617.1152	0.6	5	617.1215 ; 491.0869; 465.1078; 313.0584; 303.0520; 194.9932
27	9.682	Myricetin deoxyhexoside	C ₂₁ H ₂₀ O ₁₂	463.0882	0	12	463.0910; 317.0315; 316.0238 ; 287.0207; 316.0238; 271.0254
28	9.688	Quercetin hexoside gallate	C ₂₁ H ₂₈ O ₂₁	615.1050	−0.7	8.0	615.1046; 463.0907 ; 301.0373; 300.0281
29	10.014	Phloretin hexoside	C ₂₁ H ₂₄ O ₁₀	435.1296	−0.2	10.0	345.0967; 315.0860 ; 273.0772; 209.0455; 167.0348; 123.0450
30	10.033	Quercetin hexoside	C ₂₁ H ₂₀ O ₁₂	463.0892	2.2	12.0	463.0892; 301.0251; 300.0280 ; 271.0242
33	10.290	Patuletin hexoside	C ₂₂ H ₂₂ O ₁₃	493.0986	−0.3	12	493.1081; 331.0468; 315.0141 ; 287.0188; 271.0237; 151.0033
34	10.539	Dihydroquercetin	C ₁₅ H ₁₂ O ₇	303.0514	1.2	10.0	303.0498; 151.0409; 123.0448
35	10.870	Quercetin deoxyhexoside	C ₂₁ H ₂₀ O ₁₁	447.0936	0.7	12.0	447.0964; 300.0291 ; 271.0261; 151.0028
36	11.055	Isorhamnetin rutinoside	C ₂₈ H ₃₂ O ₁₆	623.1619	0.2	13.0	623.1675; 315.0527 ; 314.0440; 300.0264
37	11.115	Isorhamnetin deoxyhexoside	C ₂₂ H ₂₂ O ₁₂	477.1036	−0.5	12.0	331.0480; 314.0456 ; 299.0212; 271.0267
38	11.185	Naringenin gallate	C ₂₂ H ₁₆ O ₉	423.0723	0.3	15	423.0747; 299.0204; 271.0253; 258.0168 ; 243.0303
39	11.331	Trihydroxy dimethoxyflavanol hexoside	C ₂₃ H ₂₄ O ₁₃	507.1146	0.4	12	507.1195; 345.0639; 344.0559 ; 273.0418
40	11.653	Isorhamnetin pentoside	C ₂₁ H ₂₀ O ₁₁	447.0937	0.9	12	447.0936; 315.0527; 314.0440 ; 300.0285; 285.0416; 271.0245; 243.0300
42	12.035	Isorhamnetin hexoside	C ₂₂ H ₂₂ O ₁₁	461.1093	0.8	12.0	461.1110; 315.0500; 314.0433 ; 271.0240; 243.0284
43	12.315	Dihydroxy trimethoxyflavone deoxyhexoside	C ₂₃ H ₂₄ O ₁₂	491.1205	2.0	12.0	491.1244; 345.0637; 344.0558 ; 329.0323; 315.0164; 301.0367; 273.0412
45	14.507	Isokaempferide	C ₁₆ H ₁₂ O ₆	299.0559	−0.7	11.0	284.0322 ; 256.0370; 255.0286; 227.0343; 151.0038
48	14.510	Methoxyquercetin	C ₁₆ H ₁₂ O ₇	315.0512	0.6	11	315.0530; 300.0257 ; 283.0235; 271.0240; 255.0287; 151.0031
49	14.609	Dimethoxyquercetin	C ₁₆ H ₁₄ O ₈	345.0615	−0.3	11	345.0607; 330.0362; 315.0144 ; 287.0186; 259.0240; 203.0388; 171.0452

Isorhamnetin glycosides, identified based on characteristic sugar losses of 308 (rutinose—H₂O; **36**), 162 (hexose—H₂O; **42**), 146 (deoxyhexose—H₂O; **37**), and 132 Da (pentose—H₂O; **41**), were the most representative among the identified methoxyflavonoids. In fact, compounds **33**, **39**, and **43–49** were in accordance with methoxylated flavonoids, whose methylation degrees were suggested based on the number of methyl radicals lost. In particular, compounds **33**, **39**, and **43** were both methoxylated and glycosylated, whereas the other compounds were detected as aglycones. Furthermore, phloretin glucoside (**29**) and naringenin gallate (**38**) were also tentatively identified.

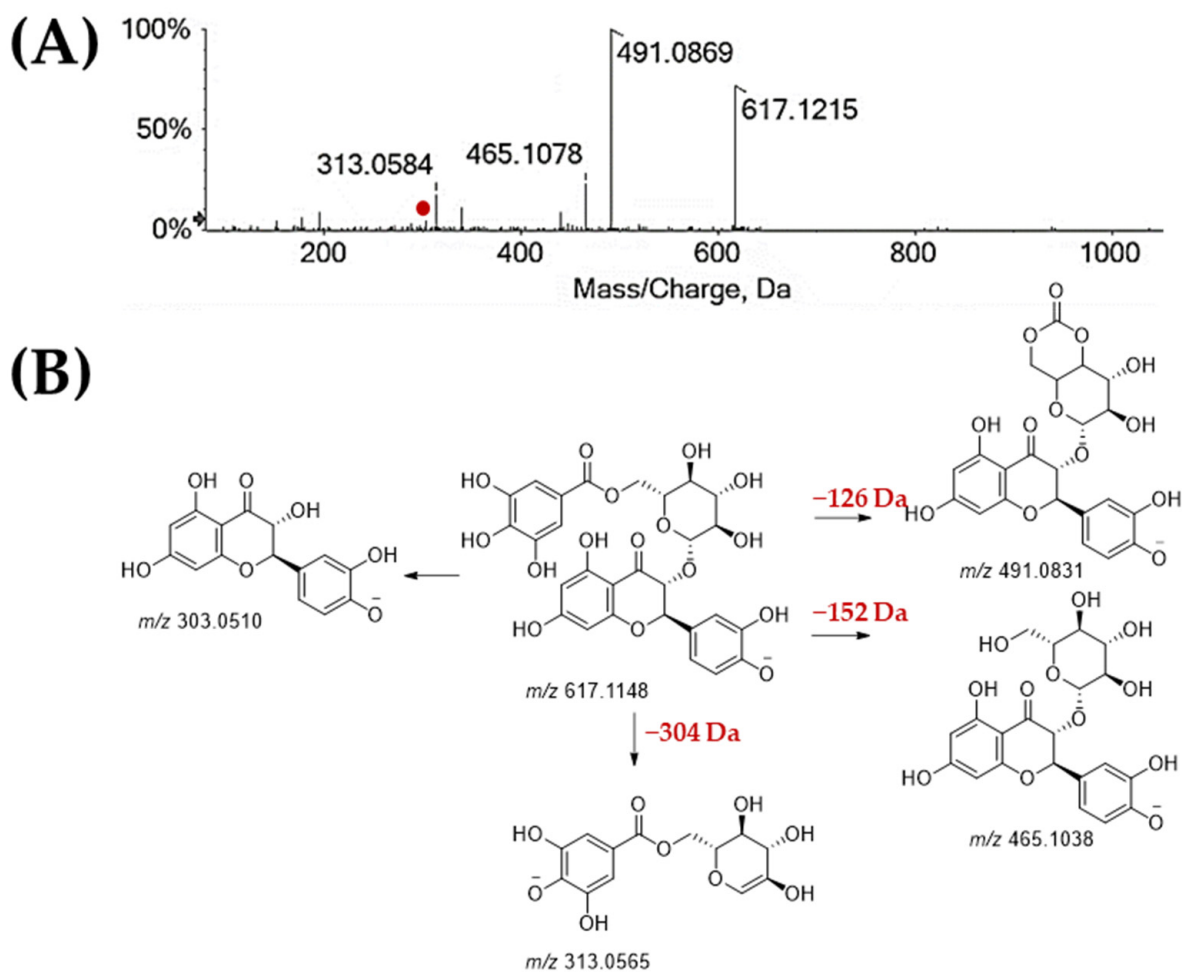


Figure 6. (A) ToF-MS/MS spectrum of the dihydroquercetin galloylhexoside (25), and (B) fragmentation pattern proposed. Theoretical mass is below each structure.

Although flavonoid occurrence was recently unraveled through an untargeted mass spectrometric analysis [43], proanthocyanidins were found as the most abundant polyphenol class both in terms of numbers and areas in E and P_{os}4, respectively, as displayed in Figure 7. Herein, probably due to the extraction strategy applied, flavonols were the most abundantly detected compounds, mainly in the outer shell (P_{os}4, P_{os}3, P_{os}2). This finding also suggests, in this case, that a fine treatment of the outer shell sample is desirable to optimize an exhaustive recovery of these compounds, which can exert a massive protective action that goes well beyond the much-claimed antioxidant activity. Long-term oral administration of myricetin demonstrated glycoregulatory activity [69], and isorhamnetin was found to reduce diabetes-related disorders by decreasing glucose levels, improving oxidative status, relieving inflammation, and modulating lipid metabolism and adipocyte differentiation [70]. Furthermore, quercetin has been investigated for treating metabolic diseases, including diabetes, hyperlipidemia, and nonalcoholic fatty liver disease [71]. These are just some of the beneficial effects enhanced by *in vitro* and *in vivo* studies on these compounds. The availability of a high quantity of waste shells in a local cultivar suggests their full recovery and the feeding of different supply chain paths with a big impact on the territory. Analogously, the presence of triterpenes (52–56) (Table 6), although negligible with respect to other detected compounds, can support the isolation of substances with a peculiar chemopreventive action. In fact, ursane-type triterpenoid saponins from the sweet chestnut heartwood were observed to be cytotoxic to prostate cancer cells and breast cancer cells [72].

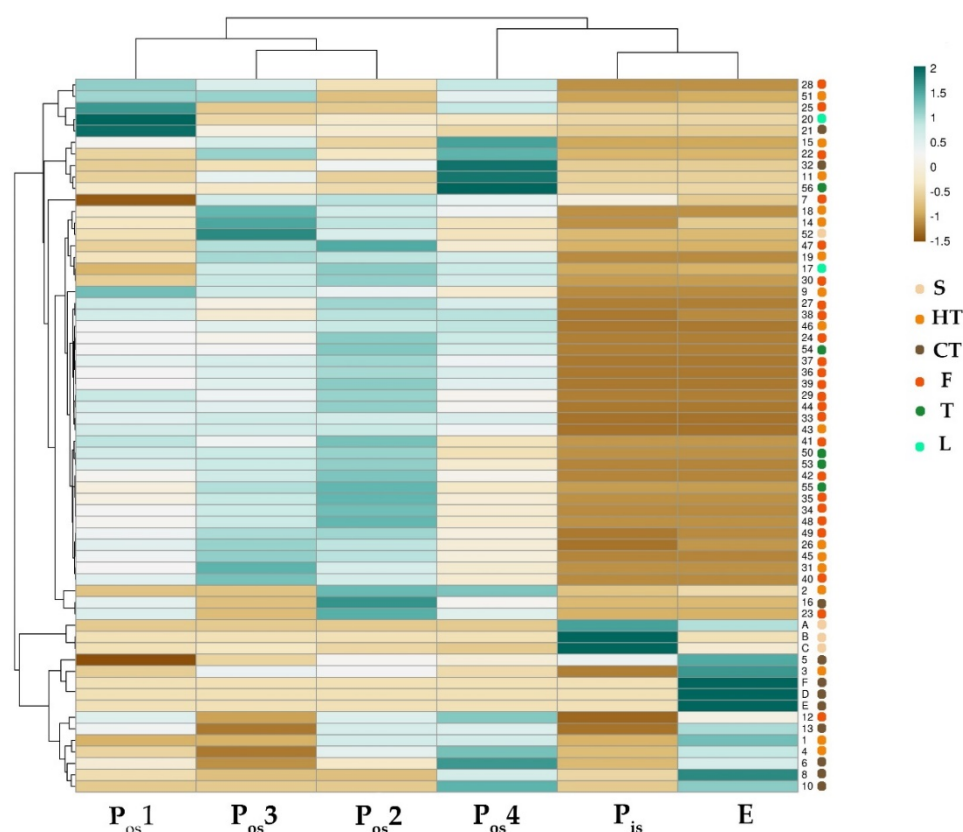


Figure 7. Heatmap of the compounds tentatively identified in the alcoholic extracts from Verdole cv. shell. S = sugars; HT = Hydrolysable Tannins; CT = Condensed Tannins; F = Flavonoids; T = Triterpenes; L = Lignans. Annotations on top of the heatmap show clustering of the investigated samples. In the ClustVis hierarchical clustering tool, both rows and columns are clustered using correlation distance and average linkage.

Table 6. UHPLC-ESI-QqToF/MS and MS/MS data useful for the tentative identification of lipid compounds in chestnut extracts (base peaks in MS/MS spectra are reported in bold; RT = retention time; RDB = ring and double bond value).

Peak	RT (Min)	Tentative Assignment	Formula	[M-H] ⁻ Found (m/z)	Error (ppm)	RDB	MS/MS Fragment Ions (m/z) and Relative Intensity (%)
50	14.665	Trihydroxyoctadecadienoic acid	C ₁₈ H ₃₂ O ₅	327.2180	0.9	3	327.2196; 229.1437; 211.1335; 171.1026
52	17.309	Chestnoside	C ₃₆ H ₅₄ O ₁₁	661.3606	1.9	10.0	661.3650 ; 499.3099; 419.2973
53	17.557	Bartogenic acid	C ₃₀ H ₄₆ O ₇	517.3182	2.2	8.0	517.3209 ; 455.3186; 437.3076
54	19.959	Dihydroxyursadienoic acid (I)	C ₃₀ H ₄₄ O ₆	499.3075	2.0	9.0	499.3075 ; 455.3160; 437.3050; 419.2946
55	19.967	Hederagenin	C ₂₉ H ₄₄ O ₅	471.3116	2.1	8.0	471.3119; 453.3013; 409.3107 ; 379.3000; 363.2712
56	20.369	Dihydroxyursadienoic acid (II)	C ₃₀ H ₄₄ O ₆	499.3065	0.1	9.0	499.3085

Relative quantitation, considering each compound area in the investigated extracts, highlights extraction is forced by the intrinsic nature of the chestnut shell part, and, for the outer shell component, by the size of the plant matrix, obtained using extraction sieves with gradually smaller dimensions. The particle size strongly influenced the extraction efficiency and the relative abundance of the compounds. In fact, the metabolic profile based on UHPLC-HRMS showed the presence of different subclasses of polyphenols, whose quantitative ratio varied between the parts of the chestnut studied.

3. Materials and Methods

3.1. Chestnut Samples

C. sativa Mill. cv. Verdole, collected in a commercial orchard located at Serino, Avellino, Italy (40°80'68.1" N; 14°89'62.9" E), was analyzed. The orchard includes 100 trees per

hectare. Morphological and phenological traits of 'Verdole' chestnut were detected on 50 trees using a guideline for the tests of distinctness, uniformity, and stability to chestnuts (*C. sativa*) TG/124/4 in agreement with UPOV (2017) [30]. Chestnut fruits were harvested on 20 October 2021. Fruits were shipped to the laboratory, checked for physical and biotic characteristics, and immediately hand-peeled to obtain the pericarp and episperm separately. The pericarp was in turn dissected into the outer and inner shells. All the samples were weighed and dried in a thermo-ventilated oven at 40 °C for 72 h and after milled using a mill (Sorvall DuPont Omni Mixer, United States). From the outer shells, using a vibrating sieving apparatus (Retsch, Haan, Germany) (53–250 µm; 250 µm–500 µm; 500 µm–1500 and >1 mm), four fractions with particles of different sizes were obtained. Each fraction was weighed and stored for further analysis.

3.2. Extraction of Verdole cv. Chestnut

Chestnut inner and outer shell samples were extracted using ethanol 96% as the extracting solvent. The sample/solvent ratio was 1:10 (3 g sample in 30 mL of solvent). Three extraction cycles were carried out by maceration interspersed with 24-h periods at 4 °C under continuous stirring. At each extraction cycle, the ethanol fraction was filtered, dried by rotavapor (Heidolph Hei-VAP Advantage, Schwabach, Germany) and then weighed to evaluate the extraction percentage yield. The samples were stored at 4 °C until further analyses.

3.3. Determination of DPPH and ABTS Radical Scavenging Capacity

The alcoholic extracts were tested towards 2,2-diphenyl-1-picrylhydrazyl (DPPH) and 2,2'-azinobis-(3-ethylbenzothiazolin-6-sulphonic acid (ABTS) for the outer pericarp (1.5, 3.125, 6.25, 12.5, 25, 50, 100 and 200.0 µg/mL final concentration levels in dimethyl sulfoxide) and for the inner pericarp and episperm (0.375, 0.75, 1.5, 3.125, 6.25, 12.5 and 25.0 µg/mL final concentration levels in water). The DPPH solution was prepared as reported by Pacifico et al. [73]. After 15 min, the absorbance at 515 nm was read using a Victor3 spectrophotometer (Perkin Elmer/Wallac; Waltham, MA, USA). ABTS was prepared as previously reported [74]. The solution was then diluted with Phosphate Buffered Saline (PBS; Gibco®, Grand Island, NY, USA; pH 7.4) to achieve an absorbance of about 0.70 at 734 nm. The extracts were incubated in ABTS solution for 6 min and the absorbance at 734 nm was detected. Trolox (4, 8, 16, 32 µM) served as the positive control in both antiradical assays. Three replicate measurements were taken for each sample (three for each concentration). The results were expressed as the effective concentration of sample required to scavenge DPPH and ABTS radicals by 50% (ID₅₀ value).

3.4. Determination of Fe (III) Reducing Power

To estimate the reducing power of the investigated alcoholic [75] the chestnut extracts (0.375, 0.75, 1.5, 3.125, 6.25, 12.5, 25.0 and 50.0 µg/mL, final) were dissolved in DMSO and in a NaH₂PO₄/Na₂HPO₄ buffer (0.2 M, pH 6.0, 2.5 mL). Samples were incubated at 50 °C for 30 min. Then, an aqueous trichloroacetic acid solution (100.0 mg/mL) was added. The tubes were placed on a shaker plate; after 10 min, 2.5 mL of the reaction mixture was taken and added to 2.5 mL of MilliQ water and 0.5 mL of ferric chloride (1.0 mg/mL). The absorbance of samples was monitored at 720 nm. The results were expressed as the effective concentration of the sample required to reduce Fe(III) by 50% (ID₅₀ value).

3.5. Determination of Total Phenols and Total Flavonoids

The Folin–Ciocalteu method was used to determine the total phenols in several extracts [76]. Each extract (1 and 0.5 mg) was added with an assay solution containing 2.25 mL of Na₂CO₃ (7.5% w/v) and 0.250 mL of the Folin–Ciocalteu reagent (FCR). Samples were stirred for 3 h at room temperature, and the absorbance was read at 765 nm by a 96-well microplate using a UV-1700 spectrophotometer (Shimadzu, Salerno, Italy). Results were expressed as milligram gallic acid equivalents (GAEs) per 100 g of dry material. Total flavonoid content (TFC) was performed using the aluminum chloride colorimetric assay [77]. Sodium nitrite

(5%, *w/v*; 0.3 mL) was first added to the samples (1 and 2 mg), previously solubilized into 5 mL of distillate water, and then AlCl₃ solution (10%, *w/v*; 0.6 mL). After 6 min, NaOH aqueous solution (1.0 M, 2.0 mL) was added, and the mixture was further diluted to 10 mL with distillate water. The absorbance was read at 510 nm against the blank (water) using a Synergy spectrophotometer (Biotek, Winooski, VT, USA). The results were expressed as milligrams of catechin equivalents per 100 g of DW.

3.6. Determination of Condensed Tannins

Condensed tannins from the different chestnut samples (outer pericarp, inner pericarp, and episperm) were determined in agreement with Porter [78]. Tannin extract was diluted in acetone 70% (*v/v*) then, butanol-HCl reagent (butanol-HCl 95:5 *v/v*) and a ferric reagent (2% ferric ammonium sulfate in HCl 2N) was added. The mixture assay was vortexed and put in a heating block at 100 °C for 60 min. The absorbance of detection was 550 nm. The results were expressed as µg/mL using catechin as standard.

3.7. UHPLC-ESI-QqTOF-MS/MS Analysis

A Shimadzu NEXERA UHPLC (Shimadzu; Tokyo, Japan) system was used with a Luna[®] Omega C18 column. A linear gradient was applied for this aim and water (A) and acetonitrile (B), both with 0.1% formic acid. Gradient conditions were as follows: 0–3 min, linear from 2 to 7% B; 3–7 min, linear from 2 to 10% B; 7–15 min, from 10 to 30% B; 15–20 min, from 30% to 45% of B; pumping 20–23 from 45% to 55%. The initial conditions were then restored at 23.01 min and allowed to re-equilibrate for 2 min. The flow rate was of 0.5 mL min⁻¹ and the injection volume of 2.0 µL. MS analysis was carried out using the AB SCIEX TripleTOF[®] 4600 (AB Sciex, Concord, ON, Canada), equipped with a DuoSpray[™] ion source, operating in ESI negative mode. The APCI probe was used for automated mass calibration using the Calibrant Delivery System (CDS). The CDS injected a calibration solution matching the polarity of ionization and calibrated the mass axis of the TripleTOF[®] system in all scan functions used (MS and/or MS/MS). The QqTOF HRMS method, which combines TOF-MS and MS/MS with Information Dependent Acquisition (IDA), consisted of a full scan TOF survey (accumulation time 250 ms, 100–1500 Da) and a maximum number of eight IDA MS/MS scans. The MS parameters were as follows: curtain gas 35 psi; nebulizer gas (GS 1) 60 psi; heated gas (GS 2) 60 psi; ion spray voltage 4.5 kV; interface heater temperature 500 °C; declustering potential –70 V. Collision Energy (CE) applied was –35 V with a CE spread of 15 V. The instrument was controlled by Analyst[®] TF 1.7 software, while data processing was carried out using PeakView[®] software version 2.2.

3.8. Statistical Analysis

All data were expressed as mean ± standard deviation (SD). The test was carried out by performing three replicate measurements for three samples (*n* = 3) of the extract (in total 3 × 3 measurements). Statistical analysis was performed using Graphpad Prism 8 software (Graphpad Software, La Jolla, CA, USA). Differences between average values were assessed based on the Tukey test at a confidence level of 95 % (*p* < 0.05). A multivariate analysis approach by ClustVis (<https://biit.cs.ut.ee/clustvis/>) was adopted to explore and clarify the quali-quantitative compositive data compounds in the chestnut waste. PCA analysis was processed using OriginPro 2015 software.

4. Conclusions

The Verdole cultivar, highly appreciated by the local communities, is an accessory cultivar from the Campania Region. Herein, a careful investigation of its agronomic traits and of bioactive compounds in the non-edible fruit parts, aimed at their recovery, was carried out. Ultrasound-assisted maceration in ethanol allowed the preparation of extracts enriched in saccharides or flavonoids, providing new insights into commonly treated matrices for the recovery of the tannic component. Since the waste of the Verdole chestnut cultivar, as well as other more or less valuable cultivars, is considerable, the depletion of the

matrices through sustainable extractions could otherwise benefit the nutraceutical sector. The comparison of the data obtained with those in the recent literature underlines the need to perform an initial agronomic evaluation of the different chestnut cultivars to define the intraparietal and interspecific variability of bioactive compounds, whose recovery, with a view to territorial sustainability, could be the starting point for new chains of value.

Supplementary Materials: The following supporting information can be downloaded at: <https://www.mdpi.com/article/10.3390/molecules27248924/s1>. Table S1. UPOV traits of *Castanea sativa* cv. Verdole.

Author Contributions: Conceptualization, M.P., A.E. and S.P. (Severina Pacifico); methodology, M.P., A.E. and S.P. (Severina Pacifico); formal analysis, M.T.P., E.F., D.C. and M.F.; investigation, M.T.P., E.F., D.C. and M.F.; data curation, M.T.P. and E.F.; writing—original draft preparation M.T.P., E.F. and S.P. (Severina Pacifico); writing—review and editing, M.P., A.E. and S.P. (Severina Pacifico); visualization, M.P., A.E., S.P. (Simona Piccolella) and S.P. (Severina Pacifico); supervision M.P., A.E. and S.P. (Severina Pacifico). All authors have read and agreed to the published version of the manuscript.

Funding: This research received no external funding.

Institutional Review Board Statement: Not applicable.

Informed Consent Statement: Not applicable.

Data Availability Statement: Data are contained within the article and Supplementary Materials.

Acknowledgments: The study was supported by the grant Research PhD programs on green and innovation issues XXXVII cycle-PON Research and Innovation REACT-EU FSE Ministerial Decree n. 1061 of 10 August 2021.

Conflicts of Interest: The authors declare no conflict of interest.

Sample Availability: Samples of the investigated extract and its fractions are available from the authors.

References

1. Beccaro, G.; Alma, A.; Bounous, G.; Gomes-Laranjo, J. *The Chestnut Handbook Crop & Forest Management*, 1st ed.; CRC Press: Boca Raton, FL, USA, 2019; p. 378.
2. Ferreira-Cardoso, J.V.; Rodrigues, L.; Gomes, E.F.; Sequeira, C.A.; Torres-Perreira, J.M.G. Lipid composition of *Castanea sativa* Mill. fruits of some native portuguese cultivars. *Acta Hort.* **1998**, *494*, 133–138. [[CrossRef](#)]
3. Gabrielli, A. La Civiltà Del Castagno. *Monti Boschi* **1994**, *65*, 3.
4. Conedera, M.; Giudici, F.; Manetti, M.C. Distribution and economic potential of the sweet chesnut (*Castanea sativa* Mill.) in Europe. *Ecol. Mediterr.* **2004**, *30*, 179–193. [[CrossRef](#)]
5. Conedera, M.; Krebs, P.; Tinner, W.; Pradella, M.; Torriani, D. The cultivation of *Castanea sativa* (Mill.) in Europe from its origin to its diffusion on a continental scale. *Veg. Hist. Archaeobot.* **2004**, *13*, 161–179. [[CrossRef](#)]
6. Romano, A.; Aponte, M. Chestnut as source of novel ingredients for celiac people. *Encycl. Food Secur. Sustain.* **2019**, *1*, 364–368.
7. Torra, M.; Belorio, M.; Ayuso, M.; Caroch, M.; Ferreira, I.C.F.R.; Barros, L.; Gómez, M. Chickpea and Chestnut Flours as Non-Gluten Alternatives in Cookies. *Foods* **2021**, *10*, 911. [[CrossRef](#)]
8. FAO. 2020. Available online: www.fao.org/statistics/en (accessed on 18 November 2022).
9. Mgaya, J.; Shombe, G.B.; Masikane, S.C.; Mlowe, S.; Mubofu, E.B.; Revaprasadu, N. Cashew nut shell: A potential bio-resource for the production of bio-sourced chemicals, materials and fuels. *Green Chem.* **2019**, *21*, 1186–1201. [[CrossRef](#)]
10. An, J.Y.; Wang, L.T.; Lv, M.J.; Wang, J.D.; Cai, Z.H.; Wang, Y.Q.; Zhang, S.; Yang, Q.; Fu, Y.J. An efficiency strategy for extraction and recovery of ellagic acid from waste chestnut shell and its biological activity evaluation. *Microchem. J.* **2020**, *154*, 105616. [[CrossRef](#)]
11. De Vasconcelos, M.C.B.M.; Nunes, F.; Viguera, C.G.; Bennett, R.N.; Rosa, E.A.S.; Ferreira-Cardoso, J.V. Industrial processing effects on chestnut fruits (*Castanea sativa* Mill.) 3. Minerals, free sugars, carotenoids and antioxidant vitamins. *Int. J. Food Sci.* **2010**, *45*, 496–505. [[CrossRef](#)]
12. Braga, N.; Rodrigues, F.; Beatriz, M.; Oliveira, P.P. *Castanea sativa* by-products: A review on added value and sustainable Application. *Nat. Prod. Res.* **2015**, *29*, 1–18. [[CrossRef](#)]
13. Pinto, D.; Vieira, E.F.; Peixoto, A.F.; Freire, C.; Freitas, V.; Costa, P.; Delerue-Matos, C.; Rodrigues, F. Optimizing the extraction of phenolic antioxidants from chestnut shells by subcritical water extraction using response surface methodology. *Food Chem.* **2020**, *334*, 127521. [[CrossRef](#)]

14. Rodriguez, C.P.; Martucci, J.F.; Neira, L.M.; Arbelaiz, A.; Eceiza, A.; Ruseckaite, R.A. Functional properties and in vitro antioxidant and antibacterial effectiveness of pigskin gelatin films incorporated with hydrolysable chestnut tannin. *Food Sci. Technol.* **2015**, *21*, 221–231. [[CrossRef](#)]
15. Turrini, F.; Donno, D.; Boggia, R.; Beccaro, G.L.; Zunin, P.; Leardi, R.; Pittaluga, A.M. An innovative green extraction and re-use strategy to valorize food supplement by-products: *Castanea sativa* bud preparations as case study. *Int. Food Res. J.* **2019**, *115*, 276–282. [[CrossRef](#)]
16. Squillaci, G.; Apone, F.; Sena, L.M.; Carola, A.; Tito, A.; Bimonte, M.; de Lucia, A.; Colucci, G.; Cara, F.L.; Morana, A. Chestnut (*Castanea sativa* Mill.) industrial wastes as a valued bioresource for the production of active ingredients. *Process Biochem.* **2018**, *64*, 228–236. [[CrossRef](#)]
17. Cacciola, N.A.; Squillaci, G.; D’Apolito, M.; Petillo, O.; Veraldi, F.; LaCara, F.; Peluso, G.; Margarucci, S.; Morana, A. *Castanea sativa* Mill. Shells Aqueous Extract Exhibits Anticancer Properties Inducing Cytotoxic and Pro-Apoptotic Effects. *Molecules* **2019**, *24*, 3401. [[CrossRef](#)]
18. Hu, M.; Yang, X.; Chang, X. Bioactive phenolic components and potential health effects of chestnut shell: A review. *J. Food Biochem.* **2021**, *4*, 13696. [[CrossRef](#)]
19. Echegaray, N.; Gómez, B.; Barba, F.J.; Franco, D.; Estévez, M.; Carballo, J.; Marszałek, K.; Lorenzo, J.M. Chestnuts and by-products as source of natural antioxidants in meat and meat products: A review. *Trends Food Sci. Technol.* **2018**, *82*, 110–121. [[CrossRef](#)]
20. Morana, A.; Squillaci, G.; Paixão, S.M.; Alves, L.; Cara, F.L.; Moura, P. Development of an energy biorefinery model for chestnut (*Castanea sativa* Mill.) shells. *Energies* **2017**, *10*, 1504. [[CrossRef](#)]
21. Zhang, Y.; Yang, Z.; Liu, G.; Wu, Y.; Ouyang, J. Inhibitory effect of chestnut (*Castanea mollissima* Blume) inner skin extract on the activity of α -amylase, α -glucosidase, dipeptidyl peptidase IV and in vitro digestibility of starches. *Food Chem.* **2020**, *324*, 126847. [[CrossRef](#)]
22. Ciucure, C.T.; Geana, E.-I.; Sandru, C.; Tita, O.; Botu, M. Phytochemical and Nutritional Profile Composition in Fruits of Different Sweet Chestnut (*Castanea sativa* Mill.) Cultivars Grown in Romania. *Separations* **2022**, *9*, 66. [[CrossRef](#)]
23. Ahmed, S.; Griffin, T.S.; Kraner, D.; Schaffner, M.K.; Sharma, D.; Hazel, M.; Leitch, A.R.; Orians, C.M.; Han, W.; Stepp, J.R.; et al. Environmental Factors Variably Impact Tea Secondary Metabolites in the Context of Climate Change. *Front. Plant Sci.* **2019**, *10*, 939. [[CrossRef](#)] [[PubMed](#)]
24. Conidi, C.; Donato, L.; Algieri, C.; Cassano, A. Valorization of chestnut processing by-products: A membrane-assisted green strategy for purifying valuable compounds from shells. *J. Clean. Prod.* **2022**, *378*, 134564. [[CrossRef](#)]
25. ISTAT. Coltivazioni: Coltivazioni Legnose Fruttifere. 2022. Available online: <http://dati.istat.it/Index.aspx?QueryId=33705> (accessed on 19 November 2022).
26. Comegna, L.; Damiano, E.; Greco, R.; Guida, A.; Olivares, L.; Picarelli, L. Effects of the Vegetation on the Hydrological Behavior of a Loose Pyroclastic Deposit. *Procedia Environ. Sci.* **2013**, *19*, 922–931. [[CrossRef](#)]
27. Protected Geographical Indication. Available online: http://data.europa.eu/eli/reg_impl/2018/1234/oj (accessed on 20 November 2022).
28. Typical Products of Campania. Available online: <http://www.agricoltura.regione.campania.it/Tipici/castagna-montella.html> (accessed on 20 November 2022).
29. Romani, A.; Campo, M.; Lagioia, G.; Scarnicci, M.C.; Paiano, A. A sustainable approach to the re-use of biomass: Synergy between circular agroindustry and Biorefinery Models. In *Industrial Symbiosis for the Circular Economy*, 1st ed.; Salomone, R., Cecchin, A., Deutz, P., Raggi, A., Cutaia, L., Eds.; Springer: Cham, Switzerland, 2020; pp. 165–179.
30. UPOV (International Union for the Protection of New Varieties of Plants). Available online: https://www.upov.int/meetings/en/doc_details.jsp?meeting_id=42485&doc_id=368806 (accessed on 7 July 2022).
31. Pérez, P.F.; López, J.F. Morphological and phenological description of 38 sweet chestnut cultivars (*Castanea sativa* Miller) in a contemporary collection. *Span. J. Agric. Res.* **2009**, *7*, 829. [[CrossRef](#)]
32. Marinoni, D.T.; Akkac, A.; Beltramo, C.; Guaraldo, P.; Boccacci, P.; Bounous, G.; Maria, A.; Ferrara, A.; Ebone, E.; Viotto, E.; et al. Genetic and morphological characterization of chestnut (*Castanea sativa* Mill.) germplasm in Piedmont (north-western Italy). *Tree Genet. Genomes* **2013**, *9*, 1017–1030. [[CrossRef](#)]
33. Prasad, K.; Hassan, F.; Yang, B.; Kong, K.; Ramanan, R.; Azlan, A.; Ismail, A. Response surface optimisation for the extraction of phenolic compounds and antioxidant capacities of underutilised mangifera pajang kosterm. peels. *Food Chem.* **2011**, *128*, 1121–1127. [[CrossRef](#)]
34. Murakami, A.N.N.; de Amboni, R.D.M.C.; Prudêncio, E.S.; Amante, E.R.; de Zanotta, L.M.; Maraschin, M.; Petrus, J.C.C.; Teófilo, R.F. Concentration of phenolic compounds in aqueous mate (*Ilex paraguariensis* A. St. Hil) extract through nanofiltration. *LWT Food Sci. Technol.* **2011**, *44*, 2211–2216. [[CrossRef](#)]
35. Aires, A.; Carvalho, R.; Saavedra, M.J. Valorization of solid wastes from chestnut industry processing: Extraction and optimization of polyphenols, tannins and ellagitannins and its potential for adhesives, cosmetic and pharmaceutical industry. *J. Waste Manag.* **2016**, *48*, 457–464. [[CrossRef](#)]
36. Chen, T.; Zhang, M.; Bhandari, B.; Yang, Z. Micronization and nanosizing of particles for an enhanced quality of food: A Review. *Crit. Rev. Food Sci. Nutr.* **2017**, *58*, 993–1001. [[CrossRef](#)]
37. Pinto, G.; de Pascale, S.; Aponte, M.; Scaloni, A.; Addeo, F.; Caira, S. Polyphenol profiling of chestnut pericarp, integument and curing water extracts to qualify these food by-products as a source of antioxidants. *Molecules* **2021**, *26*, 2335. [[CrossRef](#)]

38. Gullón, B.; Eibes, G.; Dávila, I.; Moreira, M.T.; Labidi, J.; Gullón, P. Hydrothermal treatment of chestnut shells (*Castanea sativa*) to produce oligosaccharides and antioxidant compounds. *Carbohydr. Polym.* **2018**, *192*, 75–83. [[CrossRef](#)] [[PubMed](#)]
39. Cerulli, A.; Napolitano, A.; Masullo, M.; Hošek, J.; Pizza, C.; Piacente, S. Chestnut Shells (Italian cultivar “Marrone di roccadaspide” pgi): Antioxidant activity and chemical investigation with in depth LC-hrms/MSN rationalization of tannins. *Food Res. Int.* **2020**, *129*, 108787. [[CrossRef](#)] [[PubMed](#)]
40. Vázquez, G.; Fontenla, E.; Santos, J.; Freire, M.; González-Álvarez, J.; Antorrena, G. Antioxidant activity and phenolic content of chestnut (*Castanea sativa*) shell and eucalyptus (*Eucalyptus globulus*) bark extracts. *Ind. Crops Prod.* **2008**, *28*, 279–285. [[CrossRef](#)]
41. Lameirão, F.; Pinto, D.F.; Vieira, E.F.; Peixoto, A.; Freire, C.; Sut, S.; Dall’Acqua, S.; Costa, P.; Delerue-Matos, C.; Rodrigues, F. Green-sustainable recovery of phenolic and antioxidant compounds from industrial chestnut shells using ultrasound-assisted extraction: Optimization and evaluation of biological activities in vitro. *Antioxidants* **2020**, *9*, 267. [[CrossRef](#)] [[PubMed](#)]
42. Pinto, D.; Silva, A.M.; Freitas, V.; Vallverdú-Queralt, A.; Delerue-Matos, C.; Rodrigues, F. Microwave-assisted extraction as a green technology approach to recover polyphenols from *Castanea sativa* shells. *ACS Food Sci. Technol.* **2021**, *1*, 229–241. [[CrossRef](#)]
43. Cacciola, N.A.; Cerrato, A.; Capriotti, A.L.; Cavaliere, C.; D’Apolito, M.; Montone, C.M.; Piovesana, S.; Squillaci, G.; Peluso, G.; Laganà, A. Untargeted characterization of chestnut (*Castanea sativa* Mill.) Shell polyphenol extract: A valued bioresource for prostate cancer cell growth inhibition. *Molecules* **2020**, *25*, 2730. [[CrossRef](#)]
44. Nazzaro, M.; Barbarisi, C.; Cara, F.L.; Volpe, M. Chemical and biochemical characterisation of an IGP ecotype chestnut subjected to different treatments. *Food Chem.* **2011**, *128*, 930–936. [[CrossRef](#)]
45. González López, N.; Moure, A.; Domínguez, H.; Parajó, J.C. Valorization of chestnut husks by non-isothermal hydrolysis. *Ind. Crops Prod.* **2012**, *36*, 172–176. [[CrossRef](#)]
46. Vella, F.M.; Laratta, B.; Cara, F.L.; Morana, A. Recovery of bioactive molecules from chestnut (*Castanea sativa* Mill.) by-products through extraction by different solvents. *Nat. Prod. Res.* **2017**, *32*, 1022–1032. [[CrossRef](#)]
47. Mustafa, A.M.; Abouelenen, D.; Acquaticci, L.; Alessandrini, L.; Abd-Allah, R.H.; Borsetta, G.; Sagratini, C.; Maggi, F.; Vittori, S.; Caprioli, G. Effect of roasting, boiling, and frying processing on 29 polyphenolics and antioxidant activity in seeds and shells of sweet chestnut (*Castanea sativa* mill.). *Plant* **2021**, *10*, 2192. [[CrossRef](#)]
48. Živković, J.; Mujić, I.; Nikolić, G.; Vidović, S.; Mujić, A. Extraction and analysis of condensed tannins in *Castanea sativa* Mill. *J. Cent. Eur. Agric.* **2009**, *10*, 283–290.
49. Vella, F.M.; de Masi, L.; Calandrelli, R.; Morana, A.; Laratta, B. Valorization of the agro-forestry wastes from Italian chestnut cultivars for the recovery of bioactive compounds. *Eur. Food Res. Technol.* **2019**, *245*, 2679–2686. [[CrossRef](#)]
50. Silva, V.; Falco, V.; Dias, M.I.; Barros, L.; Silva, A.; Capita, R.; Alonso-Calleja, C.; Amaral, J.S.; Iregias, G.; Ferreira, I.C.F.R.; et al. Evaluation of the phenolic profile of *Castanea sativa* Mill. by-products and their antioxidant and antimicrobial activity against Multiresistant bacteria. *Antioxidants* **2020**, *9*, 87. [[CrossRef](#)]
51. Dinis, L.; Oliveira, M.M.; Almeida, J.; Costa, R.; Gomes-Laranjo, J.; Peixoto, F. Antioxidant activities of chestnut nut of *Castanea sativa* Mill. (cultivar ‘Judia’) as function of origin ecosystem. *Food Chem.* **2012**, *132*, 1–8. [[CrossRef](#)]
52. Comandini, P.; Lerma-García, M.J.; Simó-Alfonso, E.F.; Toschi, T.G. Tannin analysis of chestnut bark samples (*Castanea sativa* mill.) by HPLC-Dad-MS. *Food Chem.* **2014**, *157*, 290–295. [[CrossRef](#)]
53. Esposito, T.; Celano, R.; Pane, C.; Piccinelli, A.L.; Sansone, F.; Picerno, P.; Zaccardelli, M.; Acquino, R.P.; Mencherini, T. Chestnut (*Castanea sativa* Miller.) burs extracts and functional compounds: UHPLC-UV-hrms profiling, antioxidant activity, and inhibitory effects on phytopathogenic fungi. *Molecules* **2019**, *24*, 302. [[CrossRef](#)]
54. Pimentel-Moral, S.; Cádiz-Gurrea, M.D.; Rodríguez-Pérez, C.; Segura-Carretero, A. Recent advances in extraction technologies of phytochemicals applied for the Revaluation of Agri-Food By-Products. In *Functional and Preservative Properties of Phytochemicals*, 1st ed.; Prakash, B., Ed.; Academic Press: San Diego, CA, USA, 2020; pp. 209–239.
55. Naczka, M.; Shahidi, F. Extraction and analysis of phenolics in food. *J. Chromatogr. A* **2004**, *1054*, 95–111. [[CrossRef](#)]
56. Ham, J.; Kim, H.; Lim, S. Antioxidant and deodorizing activities of phenolic components in chestnut inner shell extracts. *Ind. Crops Prod.* **2015**, *73*, 99–105. [[CrossRef](#)]
57. Hong, K.H. Sustainable functional finishing for cotton fabrics using chestnut shell extract. *Cellulose* **2021**, *28*, 11729–11743. [[CrossRef](#)]
58. Liu, H.; Fang, Y.; Li, Y.; Ma, L.; Wang, Q.; Xiao, G.; Zou, C. Characterization of PCS-2A, a polysaccharide derived from chestnut shell, and its protective effects against H₂O₂-induced liver injury in hybrid grouper. *Int. J. Biol. Macromol.* **2021**, *193*, 814–822. [[CrossRef](#)]
59. Jimenez, A.G.; Ellermann, M.; Abbott, W.; Sperandio, V. Diet-derived galacturonic acid regulates virulence and intestinal colonization in enterohaemorrhagic *Escherichia coli* and *Citrobacter Rodentium*. *Nat. Microbiol.* **2019**, *5*, 368–378. [[CrossRef](#)] [[PubMed](#)]
60. Wu, Y.; Zhong, Z.; Ye, Z.; Zhang, W.; He, G.; Zheng, Y.; Huang, S. D-galacturonic acid ameliorates the intestinal mucosal permeability and inflammation of functional dyspepsia in rats. *Ann. Palliat. Med.* **2021**, *10*, 538–548. [[CrossRef](#)] [[PubMed](#)]
61. Molnár, E.; Nemestóthy, N.; Bélafi-Bakó, K. Utilisation of bipolar electro dialysis for recovery of galacturonic acid. *Desalination* **2010**, *250*, 1128–1131. [[CrossRef](#)]
62. Durazzo, A.; Turfani, V.; Azzini, E.; Maiani, G.; Carcea, M. Phenols, lignans and antioxidant properties of legume and sweet chestnut flours. *Food Chem.* **2013**, *140*, 666–671. [[CrossRef](#)] [[PubMed](#)]

63. Gonçalves, B.; Borges, O.; Costa, H.S.; Bennett, R.; Santos, M.; Silva, A.P. Metabolite composition of chestnut (*Castanea sativa* Mill.) upon cooking: Proximate analysis, fibre, organic acids and phenolics. *Food Chem.* **2010**, *122*, 154–160. [[CrossRef](#)]
64. Viriot, C.; Scalbert, A.; du Penhoat, C.L.H.; Moutounet, M. Ellagitannins in woods of sessile oak and sweet chestnut dimerization and hydrolysis during wood ageing. *Phytochemistry* **1994**, *36*, 1253–1260. [[CrossRef](#)]
65. Carrero-Carralero, C.; Rodríguez-Sánchez, S.; Calvillo, I.; Martínez-Castro, I.; Soria, A.; Ramos, L.; Sanz, M. Gas chromatographic-based techniques for the characterization of low molecular weight carbohydrates and phenylalkanoic glycosides of sedum roseum root supplements. *J. Chromatogr. A* **2018**, *1570*, 116–125. [[CrossRef](#)]
66. Bai, C.; Sun, Y.; Pan, X.; Yang, J.; Li, X.; Wu, A.; Qin, D.; Cao, S.; Wenjun, Z.; Wu, J. Antitumor effects of trimethyllellagic acid isolated from *Sanguisorba officinalis* L. on colorectal cancer via angiogenesis inhibition and apoptosis induction. *Front. Pharmacol.* **2020**, *10*, 1646. [[CrossRef](#)]
67. Cerulli, A.; Masullo, M.; Mari, A.; Balato, A.; Filosa, R.; Lembo, S.; Napolitano, A.; Piacente, S. Phenolics from *Castanea sativa* leaves and their effects on UVB-induced damage. *Nat. Prod. Res.* **2017**, *32*, 1170–1175. [[CrossRef](#)]
68. Lei, L.; Chai, Y.; Lin, H.; Chen, C.; Zhao, M.; Xiong, W.; Fan, X. Dihydroquercetin activates AMPK/Nrf2/HO-1 signaling in macrophages and attenuates inflammation in LPS-induced endotoxemic mice. *Front. Pharmacol.* **2020**, *11*, 662. [[CrossRef](#)]
69. Li, Y.; Zheng, X.; Yi, X.; Liu, C.; Kong, D.; Zhang, J.; Gong, M. Myricetin: A potent approach for the treatment of type 2 diabetes as a natural class B GPCR agonist. *FASEB J.* **2017**, *31*, 2603–2611. [[CrossRef](#)] [[PubMed](#)]
70. Kalai, F.Z.; Boulaaba, M.; Ferdousi, F.; Isoda, H. Effects of isorhamnetin on diabetes and its associated complications: A review of in vitro and in vivo studies and a post hoc transcriptome analysis of involved molecular pathways. *Int. J. Mol. Sci.* **2022**, *23*, 704. [[CrossRef](#)] [[PubMed](#)]
71. Yi, H.; Peng, H.; Wu, X.; Xu, X.; Kuang, T.; Zhang, J.; Du, L.; Fan, G. The therapeutic effects and mechanisms of quercetin on metabolic diseases: Pharmacological Data and clinical evidence. *Oxid. Med. Cell. Longev.* **2021**, *2021*, 6678662. [[CrossRef](#)] [[PubMed](#)]
72. Pérez, A.J.; Pecio, Ł.; Kowalczyk, M.; Kontek, R.; Gajek, G.; Stopinsek, L.; Mirt, I.; Stochmal, A.; Oleszek, W. Cytotoxic triterpenoids isolated from sweet chestnut heartwood (*Castanea sativa*) and their health benefits implication. *Food Chem. Toxicol.* **2017**, *109*, 863–870. [[CrossRef](#)] [[PubMed](#)]
73. Pacifico, S.; Galasso, S.; Piccolella, S.; Kretschmer, N.; Pan, S.; Marciano, S.; Bauer, R.; Monaco, P. Seasonal variation in phenolic composition and antioxidant and anti-inflammatory activities of *Calamintha nepeta* (L.) savi. *Food Res. Int.* **2015**, *69*, 121–132. [[CrossRef](#)]
74. Fiorentino, M.; Gravina, C.; Piccolella, S.; Pecoraro, M.T.; Formato, M.; Stinca, A.; Pacifico, S.; Esposito, A. *Calendula arvensis* (Vaill.) L.: A Systematic Plant Analysis of the Polar Extracts from Its Organs by UHPLC-HRMS. *Foods* **2022**, *11*, 247. [[CrossRef](#)]
75. Formato, M.; Piccolella, S.; Zidorn, C.; Pacifico, S. UHPLC-HRMS Analysis of *Fagus sylvatica* (Fagaceae) Leaves: A Renewable Source of Antioxidant Polyphenols. *Antioxidants* **2021**, *10*, 1140. [[CrossRef](#)]
76. Pacifico, S.; D’Abrosca, B.; Scognamiglio, M.; D’Angelo, G.; Gallicchio, M.; Galasso, S.; Monaco, P.; Fiorentino, A. NMR-based metabolic profiling and in vitro antioxidant and hepatotoxic assessment of partially purified fractions from Golden Germander (*Teucrium polium* L.) methanolic extract. *Food Chem.* **2012**, *135*, 1957–1967. [[CrossRef](#)]
77. Formato, M.; Piccolella, S.; Zidorn, C.; Vastolo, A.; Calabrò, S.; Cutrignelli, M.I.; Pacifico, S. UHPLC-ESI-QTOF analysis and in vitro rumen fermentation for exploiting *Fagus sylvatica* leaf in ruminant diet. *Molecules* **2022**, *27*, 2217. [[CrossRef](#)]
78. Porter, L.J.; Hrstich, L.N.; Chan, B.G. The conversion of procyanidins and prodelphinidins to cyanidin and Delphinidin. *Phytochemistry* **1985**, *25*, 223–230. [[CrossRef](#)]